Title: Imbalance of Tregs/B cells and elevated complement signalling are hallmarks of refractory myasthenia gravis

Authors: Katherine C Dodd [1,2*], Kirsten Baillie [3], James KL Holt [4], M Isabel Leite [5,6], James AL Miller [7], Jennifer Spillane [8], Stuart Viegas [9], Wioleta M Zelek [3], Jon Sussman [2], Madhvi Menon [1*]

Affiliations:

[1]The Lydia Becker Institute for Immunology and Inflammation, University of Manchester

[2]Manchester Centre for Clinical Neurosciences, The Northern Care Alliance NHS Foundation Trust

[3]UK Dementia Research Institute Cardiff and Division of Infection and Immunity, School of Medicine, Cardiff University, Cardiff, Wales, United Kingdom

[4] The Walton Centre NHS Foundation Trust

[5] The University of Oxford

[6] Oxford University Hospitals NHS Foundation Trust

[7]Newcastle Hospitals NHS Foundation Trust

[8]University College London Hospitals NHS Foundation Trust

[9]Imperial College Healthcare NHS Trust

*Corresponding authors

Abstract:

Despite recent therapeutic advances in myasthenia gravis (MG), many patients remain refractory and biomarkers to help guide treatment decisions are lacking. Here, we examined circulating lymphocytes and the expression of complement receptors on T and B cells, alongside complement proteins, in patients with acetylcholine receptor antibody positive MG (sub-grouped by those: stable not on immunosuppression; stable on immunosuppression; refractory; and treatment naïve) compared to controls. Refractory patients displayed the highest frequency of memory B cells, and increased production of IL-6 and TNF-α upon toll-like receptor/ CD40 activation *in vitro*, suggesting an enhanced inflammatory phenotype. This was mirrored by a dramatic loss of regulatory T cells (Tregs) and dendritic cells in refractory disease.

Refractory MG was also characterised by higher circulating complement proteins C3, C5 and clusterin as well as increased expression of complement receptors on B and T cells, most prominently CD55 on CD8 T cells. Following B cell depletion therapy (anti-CD20), residual plasmablasts were found in circulation, likely to be drivers of ongoing disease, and highlighting the problem of therapy targeting only CD20-expressing B cells. Baseline low B cell frequency (<3%), and high complement receptor expression were associated with poor response to rituximab, suggesting that alternative treatment strategies such as complement inhibition might be more favourable in these patients.

Overall, our findings highlight an altered lymphocyte signature in patients with refractory MG and support the use of plasma cell depletion and therapies that promote Treg expansion as promising therapeutic avenues.

One Sentence Summary:

Refractory myasthenia gravis is associated with a loss of Tregs, an expansion of pro-inflammatory B cells and elevated lymphocyte complement receptor expression.

Main Text:

INTRODUCTION

In Myasthenia Gravis (MG), autoantibodies target the neuromuscular junction and cause fatigable muscle weakness. This can affect muscles of the eyes, causing ptosis and double vision (ocular MG if in isolation), as well as, in the majority of patients, muscles that are involved in facial movements, chewing and swallowing, breathing, and limb function (generalised MG). MG is a highly heterogenous disease of variable severity. A significant proportion of patients are refractory to standard immunosuppression, with resultant health complications and implications upon quality of life and large health-care resource utilization (*1*, *2*). Currently there are no prognostic biomarkers to help predict those who are likely to be refractory to standard therapies and who would benefit from early aggressive therapy.

The most common pathogenic antibody, found in around 85% of cases of MG, is targeted against the acetylcholine-receptor (AChR) (*3*). AChR-MG can be divided into three main sub-groups: (i) early-onset (EOMG), which is observed primarily in females in their third and fourth decade and is characterised by lymphoid follicular hyperplasia with germinal centres in the thymus, (ii) late-onset (LOMG), seen more commonly in males around the seventh decade, and (iii) thymoma-related. Therapy for generalised MG is initially with the acetylcholinesterase inhibitor pyridostigmine, followed by corticosteroids, and then, if necessary, steroid sparing immunosuppression with agents such as azathioprine, mycophenolate mofetil, or methotrexate, with B cell depleting agents typically used in refractory disease. Newer therapies including complement inhibition and neonatal Fc receptor (FcRn) inhibition have shown benefit (*4*), but are not yet available in the UK on the NHS. Current clinical practice involves treatment escalation by monitoring clinical symptom severity, with a lack of proven

biomarkers to predict treatment response or determine treatment efficacy in individual patients.

Previous immunophenotyping studies in MG have largely focused on disease (without sub-grouping) compared to health, resulting in difficulty interpreting the effects of disease activity and immunosuppression. MG has been shown to be T cell dependent, as mice lacking CD4 or CD8 T cells do not develop disease (*6*). Previous studies have identified an expansion of circulating T follicular helper (Tfh) cells (*5*, *6*), as well as a functional defect in regulatory T cells (Tregs) (*7*, *8*). In addition to T cells, studies comparing AChR-MG to healthy controls have reported higher levels of circulating $CD27^{hi}CD20^{lo}$ plasmablasts and $CD138^{+}$ plasma cells (*9*, *10*), and an increase in switched memory B cell subsets in non-immunosuppressed patients with generalised MG in comparison to controls (*11*). Immunosuppression in autoimmune disease has been shown to reduce naïve B cells and increase naïve T cells (*9*, *12*), but biomarkers indicative of an effective dose are lacking.

Pathophysiology of refractory disease, resistant to standard therapy, is yet to be fully elucidated. A severe form of MG is known to be triggered by immune-checkpoint inhibition (*13*), but the role these molecules play in disease is not fully understood. Programmed death ligand-1 (PD-L1) has been shown to be upregulated in muscle cells in MG (*14*), and is expressed in thymic epithelial tumours and thymic hyperplasia (*15*, *16*), but expression on circulating lymphocytes in the disease does not appear to have been studied previously. Additionally, the innate immune system is increasingly recognised as contributing to autoimmune disease pathology, and there is evidence of involvement of myeloid cells in the initiation, perpetuation, and end-organ damage seen in MG (*17*–*19*). Disruptions in dendritic cell (DC) and monocyte phenotypes have been recently been implicated in MG pathophysiology (*11*, *20*, *21*), however circulating myeloid cell frequencies are understudied in MG.

In addition to alterations to immune cell subsets, it is well known that complement plays a pivotal role in the pathogenic mechanisms of AChR-MG. AChR auto-antibodies are known to activate the complement system, leading to membrane attack complex (MAC) deposition on the muscle end plate (*23*). In AChR-MG, there is inconsistency in previous studies evaluating levels of complement proteins in patients compared to controls. Whereas some studies have reported lower serum C3 and C4 levels (*23*, *24*), more recent studies have reported either no differences or higher levels of C3, C3b and C5a in MG compared to controls (*26*, *27*). Furthermore, the interaction between the complement system and lymphocytes in MG is understudied. However, studies in other autoimmune diseases have demonstrated that B cell immune function is modulated by complement. For instance, in C3 and C4 deficient experimental autoimmune MG (EAMG) mice, there is increased B cell apoptosis due to a lack of complement stimulation (*28*). Complement receptor 2 (CD21) binds to C3d and promotes B cell survival, activation and antibody production (*29*, *30*). CD21 is strongly expressed on mature B cells, and has, perhaps unsurprisingly, been found to be increased on AChR antibody-producing B cells and correlated with AChR IgG levels in patients with MG (*30*). In contrast, B cell complement receptor 1 (CD35) binds to C3b and C4b, and promotes regulatory B cell function, with reduced expression seen on B cells in other autoimmune conditions (*32*, *33*).

Complement regulators CD55 (decay-accelerating factor; DAF), CD59 (protectin), and CD46 (membrane cofactor protein; MCP) provide negative feedback to complement activation, and are expressed by T cells. EAMG mice lacking expression of complement regulators CD55 and/or CD59 are more susceptible to disease, and display a profoundly severe phenotype, with increased levels of serum cytokines, muscle inflammation and loss of end plates (*34*, *35*). CD55, CD59 and CD46 have also been shown to modulate T cell proliferation, signalling (such as through tyrosine kinases), expression of activation markers, and secretion of cytokines,

demonstrating their wider role in immune regulation (*36*, *37*), however the expression of these makers on the T cells in MG has not previously been published.

In the era of emerging high-cost specific therapies for MG, including therapies targeting the complement system, FcRn, plasma cells and cytokines, it's more important than ever to differentiate patients that are likely to be refractory to standard therapies. Here, we undertook an observational cohort study to define immune cell profiles in refractory MG to identify biomarkers that might guide treatment decisions, and novel therapeutic targets to improve clinical outcomes.

RESULTS

Clinical Cohorts

The study recruited 61 participants with AChR-MG and 21 controls, with no other autoimmune disease that would require immunosuppression, and no solid organ or haematological cancer. Participants with AChR-MG were recruited in four specific cohorts: stable-non immunosuppressed (SNIS; stable on only low dose acetylcholinesterase inhibitors (≤120mg/day) for over two years), stable immunosuppressed (SIS; stable for over two years on azathioprine or mycophenolate mofetil (MMF) with ≤5mg/day prednisolone), refractory (eligible for rituximab as per the NHS England criteria (*38*); on corticosteroids and other immunosuppression with ongoing disease activity, or explosive bulbar onset), and treatment naïve (TN; diagnosed within the previous 6 months and not yet taking any form of immunosuppression).

All participants with MG were AChR antibody (AChR-Ab) positive at diagnosis, those with thymoma were excluded. The groups underwent immunophenotyping and comparison to age and gender matched controls with no autoimmune disease or solid organ malignancy. Four participants were excluded from analysis (one due to subsequent diagnosis of chronic myeloid leukaemia, one due to thymoma, one due to high CRP and suspicion of concurrent infection, and one control due to a grossly abnormal immune phenotype of uncertain cause). As a result, 58 participants with AChR-MG were studied: n=17 SNIS (5/17 EOMG), n=23 SIS (5/23 EOMG), n=10 refractory (4/10 EOMG), n=8 TN (2/8 EOMG), n=20 controls. Demographics and clinical features of the included participants can be seen in table 1 and Fig. 1A. Comparison of age and sex did not significantly differ between patient and control groups. AChR titre and total lymphocyte count did not differ between disease cohorts, and antibody titre did not correlate with disease severity (Fig. 1B and S1A).

Table 1. Demographics and clinical characteristics of participants.

	Control	***MG total***				
			SNIS	**SIS**	**Refractory**	**TN**
N	**20**	**58**	17	23	10	8
Age *(mean, years)*	**61.5**	**63.0**	65.1	66.7	54.5	59.8
Sex *(% female)*	**45%**	**41%**	47%	30%	50%	50%
BMI	**30.0**	**29.0**	27.6	28.9	32.7	27.6
Ethnicity						
Asian	**10%**	**6.9%**	5.9%	4.3%	10%	12.5%
Afrocaribbean	**5%**	**3.4%**	0%	4.3%	10%	0%
Caucasian	**85%**	**89.7%**	94.1%	91.3%	80%	87.5%
Disease severity *(mean, MGC / 50)*	**N/A**	**5.2**	1.1	1.2	19.7	7.25
Disease-related quality of life *(mean, MG-QoL 15r /30)*	**N/A**	**7.6**	1.1	4	22.3	13.6
Disease duration *(mean, years)*	**N/A**	**9.1**	11.0	12.3	5.3	0.36
Prednisolone dose *(mean over past 3 months, mg/day)*	**0**	**4.4**	0	0.8	23.8	0
Other Immunosuppression	**Nil**	**26% AZA** **22% MMF**	Nil	57% AZA 43% MMF	20% AZA 30% MMF	Nil

		1.7% MTX			10% MTX	
Co-morbidities						
T2DM	**10%**	**26%**	18%	30%	50%	0%
HTN	**35%**	**41%**	24%	48%	50%	50%
OA	**20%**	**9%**	6%	0%	20%	25%
Hight cholesterol	**50%**	**17%**	35%	11%	30%	25%
COPD / Asthma	**30%**	**19%**	18%	17%	20%	25%
Hypothyroidism	**5%**	**5%**	12%	0%	10%	0%
AChR-Ab titre *(median, nmol/L, normal <0.45)*	**0.23**	**14.76**	13.16	13.83	23.92	17.16
Total lymphocyte count *(median, x10^9/L, normal range 1.0-4.0)*	**1.5**	**1.4**	1.4	1.1	2.0	1.7

Abbreviations: AChR-Ab, acetylcholine receptor antibody; AZA, azathioprine; BMI, body mass index; MTX, methotrexate; MG, myasthenia gravis; MGC, MG Composite; MMF, mycophenolate mofetil; SIS, stable immunosuppressed; SNIS, stable non-immunosuppressed; TN, treatment naïve.

Expansion of memory B cells with pro-inflammatory phenotype in refractory MG

To determine if B cell frequency was a better marker of effective immunosuppression than total lymphocyte count, flow cytometry analysis of peripheral blood mononuclear cells (PBMCs) was undertaken. We observed a significant reduction in CD19 count in disease compared to controls, mainly in the SIS cohort; but this did not distinguish between those on effective immunosuppression (SIS) and those refractory to immunosuppression (Fig. 1C, gating strategy Fig. S1B). Absolute PBMC counts did not differ between cohorts (Fig. S1C).

Further analysis revealed that $CD27^{+}$ B cells were significantly expanded in disease compared to controls (Fig. 1D). Importantly, this expansion was found to be highest in the refractory cohort when comparing disease subgroups (Fig. 1D and S1D-S1E). Next, we evaluated the expression of CD38 and CD24 on B cells and found that memory B cells were expanded in patients compared to controls, again significantly in the refractory cohort (Fig. 1E-1F). When the patient cohort was grouped by age of disease onset, we observed an expansion of memory B cells and $CD27^{+}$ B cells in those with EOMG compared to LOMG; this was not associated with gender or age (Fig 1F and S1E-S1F). There was a weak positive correlation between memory B cells and disease severity (Fig. S1G).

Furthermore, we observed a reduction in mature B cells in MG patients compared to controls (Fig. 1G), however no differences were seen between MG subgroups (Fig. S1H). Both immunosuppressed groups (SIS and refractory) displayed reduction in transitional B cells (Fig. 1H), a known consequence of azathioprine and MMF (4), with no overall difference between MG patients and controls (Fig. S1I). Surprisingly, there were no differences observed in the frequency of circulating plasmablasts, when measured as $CD38^{++}CD24^{-}$, $CD38^{++}CD27^{++}$ or Blimp-1^{+} between cohorts (Fig. S1J-S1L).

Following this, we characterised B cells into naïve, switched memory, unswitched memory, and double negative memory B cell subsets based on the expression of immunoglobulin D (IgD) and CD27 (Fig. 1I). This analysis revealed an expansion of class-switched memory B cells, mirrored by reduction in naïve B cells in MG patients compared to controls (Fig. 1J and S1M-S1N). There was no significant difference in switched memory B cell frequency between EOMG and LOMG (Fig. S1N). However, we found increased IgG expression in MG compared to controls (Fig. 1K and gating S1O), with no differences in IgM expression (Fig S1O). Of note, the frequencies of unswitched and double negative memory B cells ($IgD^{-}CD27^{-}$) were comparable between patients and controls (Fig. S1P). We next examined the expression of BAFF-R and PD-L1 on B cells and did not observe any differences in relation to disease activity or treatment (Fig. S2A-S2B). Furthermore, Ki-67 expression (indicative of proliferation), was lower in the refractory cohort compared to SNIS, but no significant differences were observed between other cohorts (Fig. S2C).

Next, we stimulated PBMCs from MG patients or controls for 48 hours with CD40L, CpGB (TLR9 agonist) or R848 (TLR7 agonist), and assessed the production of cytokines. Interestingly, those with MG produced significantly more pro-inflammatory cytokine IL-6 upon activation via TLR9, TLR7 and CD40 (compared to controls), and this was highest in those with refractory disease upon CD40 activation (Fig. 1L and S2D). TNF-α production was significantly increased upon activation via TLR9 and TLR7, but not CD40, in MG patients compared to controls (Fig.1L). When comparing disease subgroups, TNF-α production upon TLR9 activation was highest in the refractory cohort (Fig. S2E). IL-10 production was increased in MG patients compared to controls only upon TLR9 activation, with no differences observed between patient subgroups (Fig. S2F). No differences were observed between those with EOMG compared to LOMG (Fig. S2D-S2F).

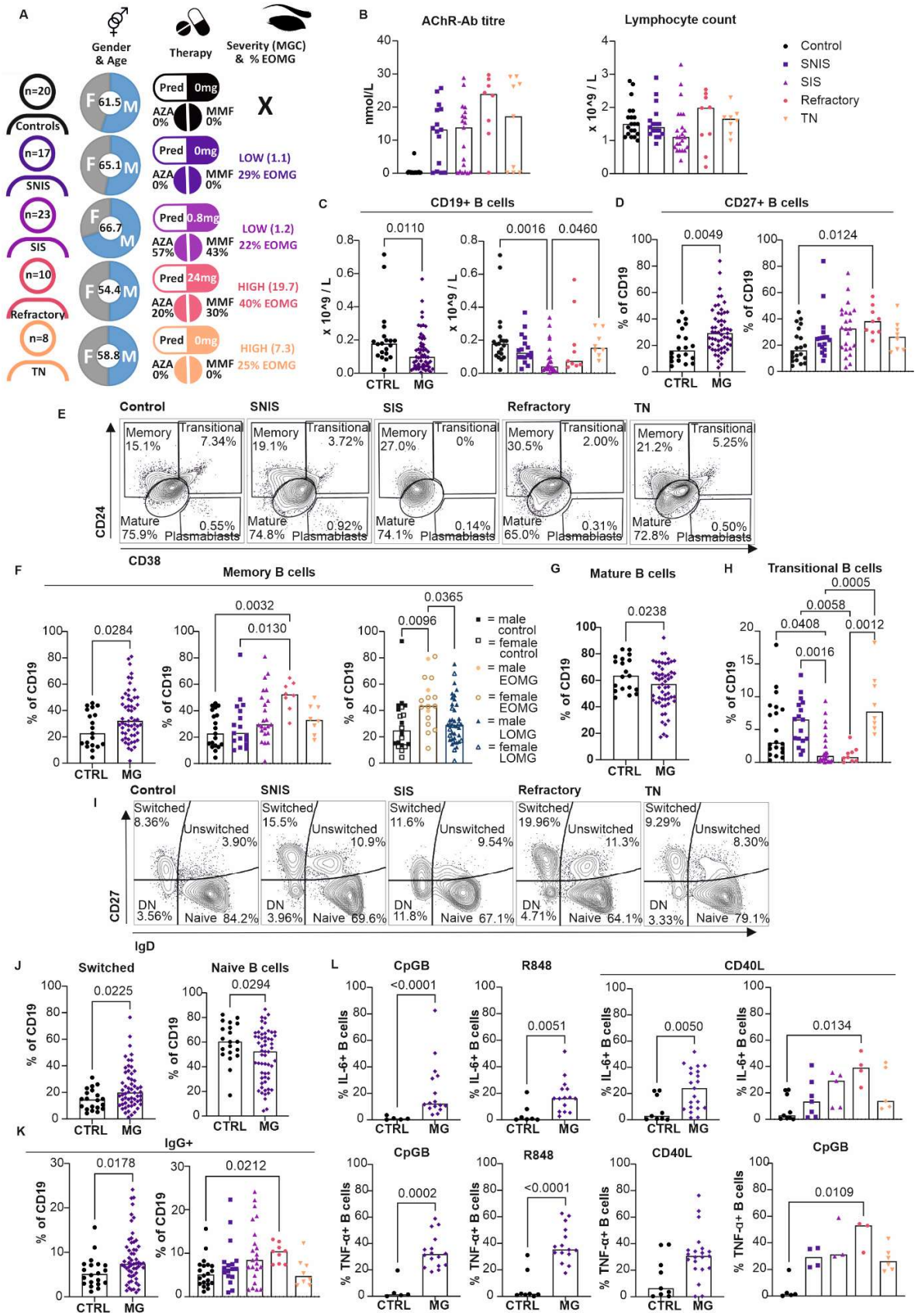
A
Gender & Age
Therapy
Severity (MGC) & % EOMG
n=20
Controls
n=17
SNIS
n=23
SIS
n=10
Refractory
n=8
TN
F 61.5 M
F 65.1 M
F 66.7 M
F 54.4 M
F 58.8 M
Pred 0mg
AZA 0%
MMF 0%
X
Pred 0mg
AZA 0%
MMF 0%
LOW (1.1)
29% EOMG
Pred 0.8mg
AZA 57%
MMF 43%
LOW (1.2)
22% EOMG
Pred 24mg
AZA 20%
MMF 30%
HIGH (19.7)
40% EOMG
Pred 0mg
AZA 0%
MMF 0%
HIGH (7.3)
25% EOMG
B
AChR-Ab titre
nmol/L
Lymphocyte count
x 10^9 / L
Control
SNIS
SIS
Refractory
TN
C
CD19+ B cells
0.0110
0.0016
0.0460
x 10^9 / L
CTRL
MG
D
CD27+ B cells
0.0049
0.0124
% of CD19
CTRL
MG
E
Control
SNIS
SIS
Refractory
TN
Memory 15.1%
Transitional 7.34%
Mature 75.9%
Plasmablasts 0.55%
Memory 19.1%
Transitional 3.72%
Mature 74.8%
Plasmablasts 0.92%
Memory 27.0%
Transitional 0%
Mature 74.1%
Plasmablasts 0.14%
Memory 30.5%
Transitional 2.00%
Mature 65.0%
Plasmablasts 0.31%
Memory 21.2%
Transitional 5.25%
Mature 72.8%
Plasmablasts 0.50%
CD24
CD38
F
Memory B cells
0.0284
0.0032
0.0130
0.0365
0.0096
% of CD19
CTRL
MG
= male control
= female control
= male EOMG
= female EOMG
= male LOMG
= female LOMG
G
Mature B cells
0.0238
% of CD19
CTRL
MG
H
Transitional B cells
0.0005
0.0058
0.0408
0.0012
0.0016
% of CD19
I
Control
SNIS
SIS
Refractory
TN
Switched 8.36%
Unswitched 3.90%
DN 3.56%
Naive 84.2%
Switched 15.5%
Unswitched 10.9%
DN 3.96%
Naive 69.6%
Switched 11.6%
Unswitched 9.54%
DN 11.8%
Naive 67.1%
Switched 19.96%
Unswitched 11.3%
DN 4.71%
Naive 64.1%
Switched 9.29%
Unswitched 8.30%
DN 3.33%
Naive 79.1%
CD27
IgD
J
Switched
0.0225
Naive B cells
0.0294
% of CD19
CTRL
MG
K
IgG+
0.0178
0.0212
% of CD19
CTRL
MG
L
CpGB
<0.0001
R848
0.0051
CD40L
0.0050
0.0134
% IL-6+ B cells
CTRL
MG
CpGB
0.0002
R848
<0.0001
CD40L
CpGB
0.0109
% TNF-α+ B cells
CTRL
MG

Figure 1.

Fig. 1. ***B cell changes in patient with MG compared to control.***

(A) Infographic showing clinical characteristics, demographics and treatment of cohorts. **(B)** AChR titre in cohorts; control (n=19), SNIS (n=15), SIS (n=19), refractory (n=8), and TN (n=9) and total lymphocyte count in cohorts; control (n=20) SNIS (n=17), SIS (n=22), refractory (n=8), and TN (n=8). **(C)** CD19 count in analysis of PBMCs and **(D)** $CD27^+$ frequency within $CD19^+$ B cells, in control (n=20) compared to MG (n=57), and between subgroups; control (n=20), SNIS (n=17), SIS (n=22), refractory (n=9), and TN (n=8). **(E)** Representative FACS plots for CD24 vs CD38, gated on $CD19^+$ live lymphocytes, for control, SNIS, SIS, refractory and TN cohorts.

(F) Memory B cell frequency within $CD19^+$ B cells in control (n=20) compared to MG (n=57), between subgroups control (n=20), SNIS (n=17), SIS (n=22), refractory (n=9), and TN (n=8), and split into early- (n=17) and late-onset MG (n=40). **(G)** Mature B cell frequency within $CD19^+$ B cells in Control (n=20) compared to MG (n=57). **(H)** Transitional B cell frequency within $CD19^+$ B cells in subgroups; control (n=20), SNIS (n=17), SIS (n=22), refractory (n=9), and TN (n=8). **(I)** Representative FACS plots displaying CD27 and IgD expression on B cells, gated on $CD19^+$ live lymphocytes, for control, SNIS, SIS, refractory and TN cohorts. **(J)** Switched and naïve (IgD^+CD27^-) B cells and **(K)** IgG^+ B cell frequency within $CD19^+$ B cells, in control (n=20) compared to MG (n=57), and between subgroups; control (n=20), SNIS (n=17), SIS (n=22), refractory (n=9), and TN (n=8) (K). **(L)** IL-6 and TNF-α positive B cells following stimulation with CPGB, R848 and CD40L in control (n=5 CPGB, n=7 R848, n=10 CD40L) compared to MG (n=16 CPGB, n=15 R848, n=23 CD40L), IL-6 positive B cells following CD40L between subgroups; control (n=10), SNIS (n=7), SIS (n=5), refractory (n=4), and TN (n=5), and TNF- α positive B cells following CpGB between subgroups; control (n=5), SNIS (n=4), SIS (n=3), refractory (n=3), and TN (n=6).

Flow cytometry was performed on peripheral blood mononuclear cells (PBMCs). Graphs show individual participant data, with bar representing median values. All comparisons are performed by student's t-test or one-way ANOVA with Tukey multiple comparison test (parametric data) or Mann-Whitney or Kruskal-Wallis with Dunn's multiple comparison test (non-parametric).

Reduced frequencies of Tregs and dendritic cells in refractory MG

To determine if these B cell changes, or disease phenotype, may relate to changes in the T cell compartment, the T cell profile was analysed. CD3 count did not differ between groups (Fig. 2A), but CD4 frequency was higher in MG patients compared to controls, mainly in those on immunosuppression (Fig. 2B and S3A-S3B). $CD8^+$ T cell frequencies did not significantly differ (Fig. S2C), but $CD4^+CD8^+$ double positive T cells were lower in MG, particularly in the SIS cohort (Fig. S3D).

When examining the CD4 T cell phenotype, naïve T cells were found to be highest in those with refractory MG (Fig. 2C and S3E-S3F). Effector memory T cells were reduced in both immunosuppressed groups (SIS and refractory), but central memory and TD effector cell frequencies did not significantly differ between the patient subgroups (Fig. 2C and S3E-S3F). Notably, regulatory T cells (Tregs), defined as $CD4^+FoxP3^+CD25^+$ T cells, were significantly reduced in the refractory cohort compared to the control and SNIS cohorts (Fig. 2D-2F). Treg frequencies negatively correlated with disease severity and disease-related quality of life scores (Fig. 2E and S3G), highlighting a potential role in ameliorating disease. As Tregs are known to suppress pro-inflammatory B cells, we next examined whether the loss of Tregs was

associated with the expansion of effector B cells. Indeed, we observed a significant negative correlation between IL-6-producing B cells and Treg frequencies (Fig. 2E). Of note, there was no difference in Treg frequencies between EOMG and LOMG (Fig. S3H). Previous studies have found expanded circulating Tfh cells frequencies in MG (*5*, *6*), however, here we observed a trend towards reduction in MG patients compared to controls, mainly in the refractory cohort (Fig. 2G and S3I).

Further, we examined the expression of immune checkpoint molecules, PD-1 and cytotoxic T lymphocyte antigen 4 (CTLA-4), as anti-PD-1 or anti-CTLA-4 therapy in cancer treatment has been shown to cause an MG-like syndrome (*13*). Moreover, genomic studies have found strong association signals at the CTLA-4 gene with MG (*38–40*). PD-1 and CTLA-4 expression by $CD4^+$ T cells, $CD8^+$ T cells or $CD4^+CD25^+FoxP3^+$ Tregs did not significantly differ between MG patient cohorts and controls (Fig S3J-S3K).

Given the complex interplay between the adaptive and innate immune systems, we next examined whether changes in myeloid cells might also influence the low Treg frequencies in refractory disease (gating strategy in Fig. S4A). Although there were no differences in DC frequencies between all MG patients and controls, there was a dramatic reduction in the refractory MG cohort when comparing disease subgroups (Fig. 2H). Next, when examining DC subtypes, we observed a reduction in both pDC and mDC frequencies in the refractory cohort (Fig. S4B). However, no differences in the pDC:mDC ratio were observed. Treg frequency does not correlate with DC frequency, but does show weak correlation with pDC frequency (Fig. S4D). Of note, pDC frequency also showed greater correlation with disease severity and quality of life scores than total DC frequency (Fig. S4D). Monocytes were expanded throughout the MG patient cohorts (apart from SNIS), and demonstrated a shift towards the classical phenotype (Fig. 2H and S4E-S4F). NK cell frequencies and subsets did not show any

significant differences between MG patients and control, or between patient cohorts (Fig. S5A-S5C). When examining the expression of CD80 and CD86 on myeloid cells, the SIS group demonstrated reduced frequencies of $CD86^+$ monocytes and DCs, but there was no difference in CD86 expression on NK cells, and no discernible difference in CD80 expression on any of the cell types examined (Fig. S5D-S5E).

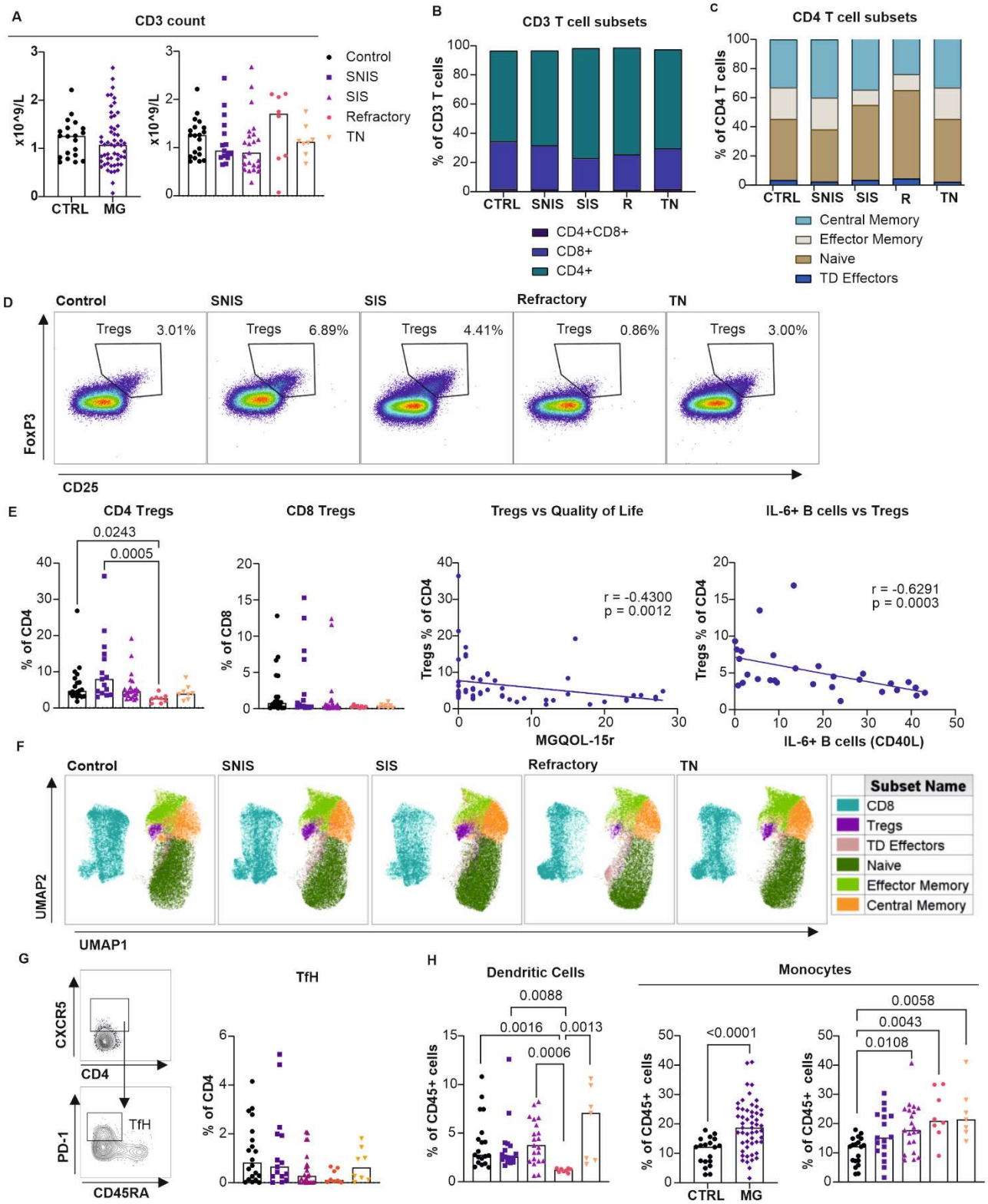
A
CD3 count
x10^9/L
CTRL
MG
Control
SNIS
SIS
Refractory
TN
B
CD3 T cell subsets
% of CD3 T cells
CTRL
SNIS
SIS
R
TN
CD4+CD8+
CD8+
CD4+
C
CD4 T cell subsets
% of CD4 T cells
Central Memory
Effector Memory
Naive
TD Effectors
D
Control
SNIS
SIS
Refractory
TN
Tregs 3.01%
Tregs 6.89%
Tregs 4.41%
Tregs 0.86%
Tregs 3.00%
FoxP3
CD25
E
CD4 Tregs
0.0243
0.0005
% of CD4
CD8 Tregs
% of CD8
Tregs vs Quality of Life
r = -0.4300
p = 0.0012
Tregs % of CD4
MGQOL-15r
IL-6+ B cells vs Tregs
r = -0.6291
p = 0.0003
IL-6+ B cells (CD40L)
F
Control
SNIS
SIS
Refractory
TN
UMAP2
UMAP1
Subset Name
CD8
Tregs
TD Effectors
Naive
Effector Memory
Central Memory
G
CXCR5
CD4
PD-1
CD45RA
TfH
% of CD4
H
Dendritic Cells
0.0088
0.0016
0.0013
0.0006
% of CD45+ cells
Monocytes
<0.0001
0.0058
0.0043
0.0108
CTRL
MG

Figure 2.

Fig. 2. ***T cell alterations in patients with AChR-MG compared to controls.***

(A) CD3 count, gated on live lymphocytes in PBMCs, in control (n=20) compared to MG (n=54), and between subgroups; control (n=20), SNIS (n=15), SIS (n=23), refractory (n=8), and TN (n=8). **(B)** Proportion of $CD4^+$, $CD8^+$ and $CD4^+CD8^+$ cells, within $CD3^+$ live lymphocytes, and **(C)** naïve, central and effector memory, and TD effector T cell frequency, gated on $CD4^+$ T cells, in control (n=20), SNIS (n=15), SIS (n=23), refractory (n=8), and TN (n=8). **(D)** Representative FACS plots for Tregs in control, SNIS, SIS, refractory and TN cohorts. **(E)** $FoxP3^+CD25^+$ Treg frequency, gated on both $CD4^+$ and $CD8^+$ T cells, in control (n=20), SNIS (n=15), SIS (n=23), refractory (n=8), and TN (n=8). Simple linear regression for CD4 Treg frequency against MG Quality of Life-15 revised (QoL-15r) score (n=54) and IL-6^+ B cells when stimulated with CD40L (n=29). **(F)** UMAP plots demonstrating main T cell subsets in representative selection of 5,000 $CD3^+$ live lymphocytes of control (n=8), SNIS (n=8), SIS (n=8), refractory (n=8) and TN (n=8). **(G)** FACS plot demonstrating gating of $CXCR5^+CD45RA^-PD\text{-}1^+$ Tfh cells, gated on $CD4^+$ T cells, and graph showing $CXCR5^+CD45RA^-PD\text{-}1^+$ Tfh cell frequency count in control (n=20), SNIS (n=15), SIS (n=23), refractory (n=8), and TN (n=8). **(H)** Frequencies of dendritic cells ($CD3^-CD19^-CD66b^-CD14^-HLA\text{-}DR^+$) in subgroups control (n=18), SNIS (n=17), SIS (n=19), refractory (n=6), TN (n=6), and monocytes ($CD3^-CD19^-CD66b^-CD14^+HLA\text{-}DR^+CD64^+$) in control (n=18) compared to MG (n=48) and in subgroups. Flow cytometry was performed on peripheral blood mononuclear cells (PBMCs). Graphs show individual participant data, with bar representing median values. All comparisons are performed by student's t-test or one-way ANOVA with Tukey multiple comparison test (parametric data) or Mann-Whitney or Kruskal-Wallis with Dunn's multiple comparison test (non-parametric). Correlation is calculated by Pearson (parametric) or Spearman correlation.

Complement receptor expression on lymphocytes and circulating complement proteins are elevated in refractory MG

Knowing that AChR antibodies activate the complement system (*42*), we next examined the circulating levels of complement proteins (proteins TCC, Ba, C1q, C4, C9, CR1, FH, FHR4, FI, iC3b, properdin, and FHR125) in MG and its association with disease and treatment. This analysis revealed that although there were no different observed when comparing all MG patients to controls, the circulating levels of C3, C5 and clusterin were significantly elevated in refractory disease when comparing patient subgroups (Fig. 3A-3B and S6A-S6C). Further, the levels of C3, C5 and clusterin positively correlated with disease severity and quality of life scores (Fig. 3C, S6D-S6E).C3, C5 and clusterin levels did not differ between EOMG and LOMG (Fig. S6F).

Complement is known to cause disruption at the neuromuscular junction, contributing to loss of neuromuscular transmission (*28*), however, the interaction with lymphocytes in autoimmunity is poorly understood. To explore this, we examined complement receptor 1 (CD21) and 2 (CD35) on B cells, and discovered that the expression of both receptors (as measured by mean fluorescence intensity) was increased in MG patients compared to controls (Fig. 3D). However, frequencies of CD35-expressing B cells, but not CD21-expressing B cells, were overall lower in MG patients compared to controls, with no differences observed between patient subgroups (Fig. S7A).

We next examined the expression of three complement receptors on T cells: CD55, CD46, and CD59 (Fig. S7B). Intensity of expression of CD55 and CD46, but not CD59, was significantly higher on CD4 and CD8 T cells (Fig. 3E). When examined by treatment subgroups, CD55 expression was found to be highest in the refractory cohort on CD8 T cells, and in both refractory and SIS cohorts on CD4 T cells (Fig. 3F-3G, and S7C), however. there was no

significant difference in intensity of expression of CD46 between subgroups (Fig S7D). When assessing frequencies, we observed a significant expansion of CD55-expressing CD4 and CD8 T cells, and CD46-expressing CD4 T cells in MG patients compared to controls (Fig. S7E). No differences were observed in CD59-expressing T cells. When comparing patient cohorts, $CD55^+$ and $CD46^+$ CD8 T cell frequencies were found to be highest in the refractory cohort (Fig. 3F and S7F-S7G) indicating ongoing complement-mediated pathology in refractory disease.

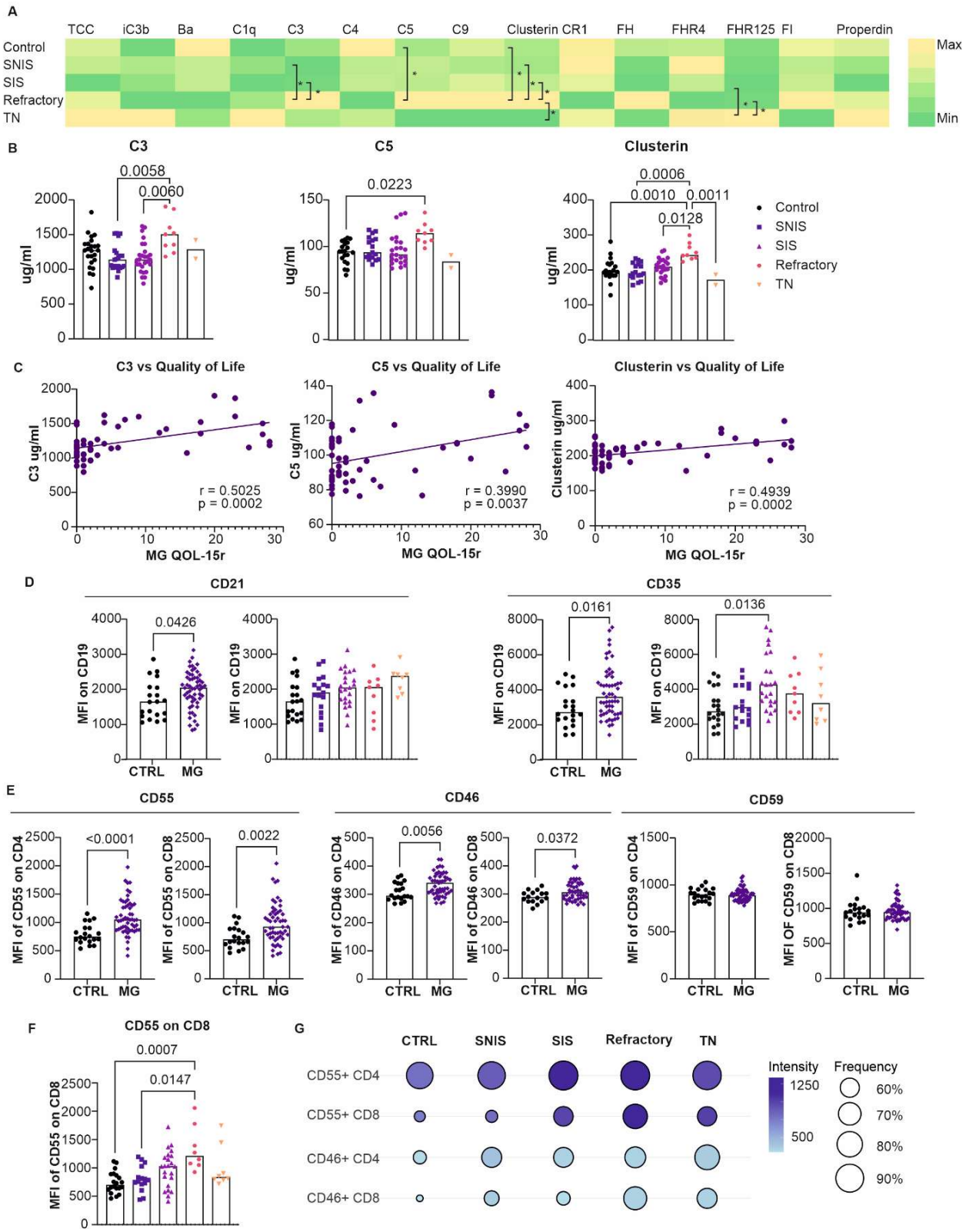
A
TCC
iC3b
Ba
C1q
C3
C4
C5
C9
Clusterin
CR1
FH
FHR4
FHR125
FI
Properdin
Control
SNIS
SIS
Refractory
TN
Max
Min
B
C3
C5
Clusterin
ug/ml
0.0058
0.0060
0.0223
0.0006
0.0010
0.0011
0.0128
Control
SNIS
SIS
Refractory
TN
C
C3 vs Quality of Life
C5 vs Quality of Life
Clusterin vs Quality of Life
C3 ug/ml
C5 ug/ml
Clusterin ug/ml
r = 0.5025
p = 0.0002
r = 0.3990
p = 0.0037
r = 0.4939
p = 0.0002
MG QOL-15r
D
CD21
CD35
MFI on CD19
0.0426
0.0161
0.0136
CTRL
MG
E
CD55
CD46
CD59
MFI of CD55 on CD4
MFI of CD55 on CD8
MFI of CD46 on CD4
MFI of CD46 on CD8
MFI of CD59 on CD4
MFI OF CD59 on CD8
<0.0001
0.0022
0.0056
0.0372
F
CD55 on CD8
MFI of CD55 on CD8
0.0007
0.0147
G
CTRL
SNIS
SIS
Refractory
TN
CD55+ CD4
CD55+ CD8
CD46+ CD4
CD46+ CD8
Intensity
1250
500
Frequency
60%
70%
80%
90%

Figure 3.

Fig. 3*. Circulating complement proteins, and complement receptors on lymphocytes.*

Complement proteins were measured by ELISA and their receptor expression on PBMCs analysed by flow cytometry. **(A)** Heatmap demonstrating relative concentration of each complement protein analysed and **(B)** frequencies of C3, C5, and clusterin in subgroups; control (n=20), SNIS (n=18), SIS (n=23), Refractory (n=9), and TN (n=2). **(C)** Correlation between C3, C5, clusterin and quality of life (MG Qol-15r score) (n=52). **(D)** Expression of CD21 and CD35 on B cells in control (n=20) compared to MG (n=56), and between subgroups; control (n=20), SNIS (n=17), SIS (n=22), refractory (n=9), and TN (n=8). **(E)** Graphs showing expression of CD55, CD46 and CD59 on CD4 and CD8 T cells in control (n=20), compared to MG (n=54). **(F)** CD55 expression on CD8 T cells in subgroups; control (n=20), SNIS (n=15), SIS (n=23), refractory (n=8), and TN (n=8). **(G)** Bubble plot demonstrating frequency and intensity of expression of CD46 and CD55 on CD4 and CD8 T cells in subgroups control (n=20), SNIS (n=15), SIS (n=23), refractory (n=8), and TN (n=8). Graphs show individual participant data, with bar representing median values. All comparisons are performed by student's t-test or one-way ANOVA with Tukey multiple comparison post-test (parametric data) or Mann-Whitney or Kruskal-Wallis with Dunn's multiple comparison post-test (non-parametric). Correlation is calculated by Pearson (parametric) or Spearman correlation. Significant differences are indicated by stated p values or *=p≤0.05.

Low baseline B cell frequency predicts poor response to rituximab

Eight of the 10 refractory participants were followed up at 1-, 7- and 13-months following B cell depletion with two infusions of rituximab (or biosimilar) 1g intravenously, two weeks apart. Some of these participants were given additional doses of rituximab at the clinician's discretion; the timing of these doses, and changes in participant disease severity, quality of life, and prednisolone dose can be seen in Fig. 4A. No changes in AChR titres were observed (Fig. S8A). All participants showed successful B cell depletion, with some participants displaying partial repopulation by month 13 (Fig. 4B-4C). Notably, those who did not reduce their severity score by 50% or more (defined as non-responders; R2, R4 and R7) had baseline B cell frequencies under 3%, whereas responders had baseline frequencies above 3%. Non-responders also had longer disease duration (median of 15 years), compared to responders (1 year).

Of the remaining B lineage cells in circulation during depletion, a high proportion of these were found to be plasmablasts, alongside increased Blimp-1 expression (Fig. 4D-4E and S8A). In agreement with previous findings (*43*), the repopulating B cells (in months 7-13) were found to be transitional ($CD24^{++}CD38^{++}$) and mature ($CD24^{+}CD38^{+}$) B cells (Fig. 4D-4F). Residual B cells following depletion expressed less BAFF-R, CD21 and CD35, but not CD27 (Fig. S8A-S8B). Treg frequencies increased following B cell depletion in both responders and non-responders (Fig. 4G-4H). There were no significant changes in CD4 or CD8 T cell frequencies, T cell phenotype, or expression of PD-1 or CD55 (Fig. S8C-S8E). It is noteworthy to mention that the rituximab clinical non-responders had the highest expression of CD55 on CD8 T cells at all time-points (before and after rituximab treatment), suggesting that there was ongoing complement-mediated pathology driving disease (Fig. 4G). However, levels of C3, C5 and clusterin were unaltered in response to rituximab (Fig. S8F-S8G). In the myeloid compartment,

there was no change to DC or monocyte frequencies, but a trend to increasing NK cell frequencies (Fig. S8H).

Next, in order to examine the effect of steroid treatment, we studied treatment naïve patients at baseline and 6-month follow-up to examine differences in those given steroid treatment. Seven of the eight treatment naïve participants were followed up at 6 months, with two of these on corticosteroid therapy at follow-up, one of these alongside azathioprine. All demonstrated stability or improvement in their disease severity, and all but one in quality-of-life score (Fig. S9A-B). One participant continued to have a moderate MG composite score of 11; they had declined steroid therapy. Although the sample size is small, those who initiated steroid therapy had the greatest $CD27^+$, Blimp-1^+, IgG^+ and double negative B cell frequency at follow-up, alongside the lowest level of Tregs (Fig. S9B). These potential effects of steroids warrant further investigation in a larger patient cohort. There were no clear differences in B or T cell frequency, or expression of CD35 on B cells or CD55 on T cells, though all participants appeared to have a reduction in CD21 expression at 6 months (Fig. 9B).

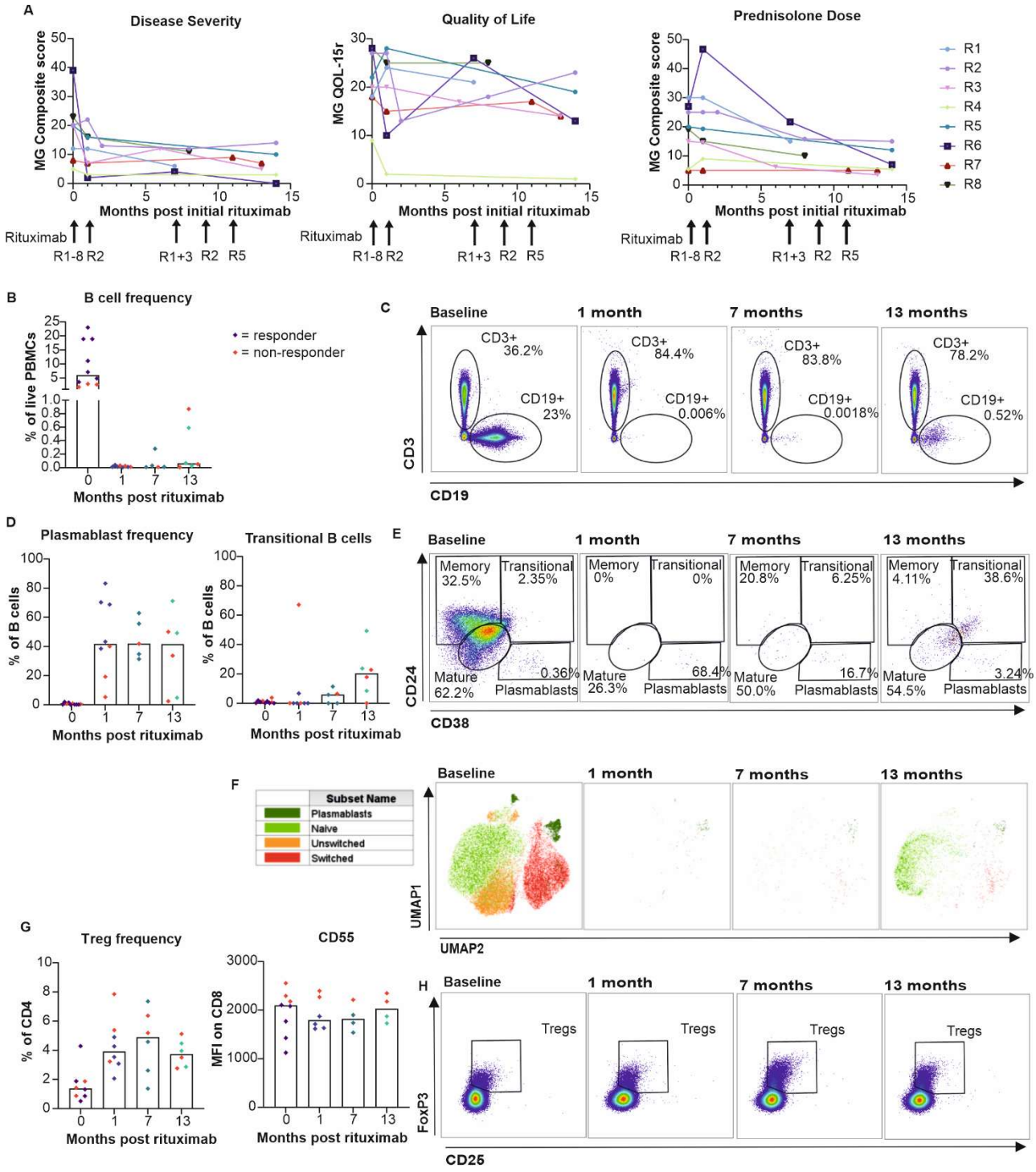
A
Disease Severity
MG Composite score
Months post initial rituximab
Rituximab
R1-8 R2
R1+3 R2 R5
Quality of Life
MG QOL-15r
Prednisolone Dose
R1
R2
R3
R4
R5
R6
R7
R8
B
B cell frequency
% of live PBMCs
= responder
= non-responder
Months post rituximab
C
Baseline
1 month
7 months
13 months
CD3+ 36.2%
CD19+ 23%
CD3+ 84.4%
CD19+ 0.006%
CD3+ 83.8%
CD19+ 0.0018%
CD3+ 78.2%
CD19+ 0.52%
CD3
CD19
D
Plasmablast frequency
Transitional B cells
% of B cells
Months post rituximab
E
Memory 32.5%
Transitional 2.35%
Mature 62.2%
0.36% Plasmablasts
Memory 0%
Transitional 0%
Mature 26.3%
68.4% Plasmablasts
Memory 20.8%
Transitional 6.25%
Mature 50.0%
16.7% Plasmablasts
Memory 4.11%
Transitional 38.6%
Mature 54.5%
3.24% Plasmablasts
CD24
CD38
F
Subset Name
Plasmablasts
Naive
Unswitched
Switched
UMAP1
UMAP2
G
Treg frequency
% of CD4
CD55
MFI on CD8
H
Tregs
FoxP3
CD25

Figure 4.

Fig. 4*. Changes following B cell depletion or corticosteroids.*

(A) Disease severity, quality of life and prednisolone dose changes following rituximab therapy. Timing of additional doses indicated by arrows. Flow cytometry was performed on peripheral blood mononuclear cells (PBMCs) at baseline (n=10), 1 month (n=8), 7 months (n=5), and 13 months (n=6) post rituximab in the refractory group. **(B)** Changes in B cell frequency. **(C)** Representative FACS plots showing changes in B and T cell frequency. **(D)** Plasmablast and transitional B cell frequency. **(E)** Representative FACS plots showing changes in B cell subsets. **(F)** UMAP plots displaying main B cell populations in all $CD19^+$ live lymphocytes (total=195,944 cells). **(G)** Changes in Treg frequency and CD55 expression on CD8 T cells. **(H)** Representative FACS plots showing changes in Treg frequencies, gated on $CD4^+$ T cells. All graphs show individual participant data, with bar representing median values.

DISCUSSION

In MG, a proportion of patients remain refractory to therapy, and biomarkers to predict disease course and thus to guide treatment decisions are lacking. This study explored circulating immune profiles in MG patients with differing treatment requirements against age- and gender-matched controls, and has identified several alterations to lymphocyte subsets and markers of complement activation that characterise refractory disease.

Circulating B cell frequencies are known to reduce with immunosuppression, or longstanding autoimmune disease (*9*), a finding we replicate here. We demonstrate that the B cell compartment in those with MG contains higher frequencies of class-switched memory B cells, particularly in refractory disease. An expansion of memory B cells has been previously reported in generalized MG compared to ocular MG and controls (*43*), with recent single cell

mapping demonstrating an increase in switched memory B cell subsets (*11*). Here, we report that the expansion of memory B cells is in EOMG rather than LOMG, which may translate to differences in response to B cell-targeted therapies.

Surprisingly, we observed no differences in circulating plasmablast frequencies. This may be because AChR auto-antibodies are thought to be mainly produced by long-lived plasma cells, which reside in the bone marrow or lymphoid tissue rather than in circulation (*42*, *45*). However, one previous study identified elevated plasmablast cell frequency in AChR-MG, defining these as CD19+CD3-CD14-CD27^{high}CD20^{low} (*9*), and another found higher frequency of circulating CD138^{+} plasma cells in patients with non-immunosuppressed AChR-MG compared to healthy controls, more so in generalised compared to ocular MG (*10*). These differences could be due to heterogenous patient population, varying treatment strategies and markers used to identify plasmablasts/ plasma cells.

Although the main immune pathology in MG is thought to be a consequence of AChR-Abs at the neuromuscular junction, we found that there is a broader inflammatory phenotype in the circulation, with B cells primed to produce pro-inflammatory cytokines IL-6 and TNF-α. This was seen in both EOMG and LOMG. IL-6 promotes plasma cell differentiation, and autoantibody production as well as inhibiting the formation of Tregs, with self-amplification through the IL-6 amplifier loop involving STAT3 and NF-κB (*46*). Conversely, Tregs are known to suppress pro-inflammatory B cell responses and promote regulatory B cell differentiation (*47*). In line with this, we found that IL-6^{+} B cell frequency correlated inversely with Treg frequencies, which were significantly reduced in refractory disease, in keeping with a previous study (*48*). Treg frequencies also correlated with disease severity and quality of life scores and therefore are a potential biomarker for disease activity.

In addition, we also identify a reduced frequency of DCs in refractory MG. A previous study showed decreased frequencies of pDCs, known to promote Treg differentiation (*49*), in treatment naive MG patients compared to healthy controls, with a reduced pDC:mDC ratio (*49*). Whilst a change in pDC:mDC ratio was not observed within our patient cohort, we observed a reduction in circulating pDCs and mDCs in refractory disease. pDC frequency also correlated with Treg frequencies, and inversely with disease severity and quality of life scores in MG patients. This is in contrast to a recent study reporting higher frequencies of circulating pDCs and mDCs in MG compared to control (*20*). Notably, that study contained an overwhelming majority of patients with mild disease (MGFA class I cases), with low numbers of those with severe disease.

In agreement with previous findings, our data shows no differences in the frequency of naïve, memory, or effector T cells in patients with MG compared to controls, in relation to treatment or severity (*50*). However, in contrast to other studies reporting an expansion of Tfh cells, we observe a nominal reduction in patients compared to controls (*6*). The prior study defined Tfh as $CD3^{+}CD4^{+}CXCR5^{+}$ cells, whereas we defined Tfh cells more robustly as $CD3^{+}CD4^{+}CXCR5^{+}CD45RA^{-}PD\text{-}1^{+}$ cells. This subset comprises a small population of the circulating T cells, and changes seen in the circulation may not correspond to those in lymphoid organs.

Expansion of monocytes was seen in disease compared to controls, particularly in those with ongoing symptoms. Increased circulating classical monocyte frequencies may be promoting ongoing MHC-II antigen presentation, but also have roles in inflammatory cytokine secretion and promotion of B cell survival (*51*). Both monocytes and DCs displayed reduced CD86 expression in those stable on immunosuppression, for monocytes this distinguished them from those who had not responded to immunosuppression (the refractory group). CD86 is the

ligand for CD28 and CTLA-4 on T cells, and therefore reduced expression of CD86 may result in impaired T cell activation and regulatory function (*52*).

There has been recent interest in the role of NK cells in MG. A previous study showed elevated frequencies of NK cells in those in remission compared to disease exacerbation and controls (*53*). In agreement with this study, we report a trend to higher frequencies of NK cells in the SNIS cohort, suggesting they may play a protective role. Furthermore, other studies demonstrated a reduction in $CD56^{+}CD16^{+}$ NK cells, which correlated negatively with disease severity (*11*), and an expansion of CD56dimCD16dim/- NK cells in MG patients with a high disease burden, due to prior ADCC activity (*54*). However, we did not identify differences in NK cell subsets, perhaps due to differences in therapies.

Circulating levels of total C3, C5, and the inhibitory molecule clusterin were elevated in the refractory cohort, correlating positively with disease severity and quality of life scores, positioning them as additional potential biomarkers of disease activity. Although, other studies have reported varying results of complement levels, this might be contributed to by a number of confounding factors, including laboratory methodology and participant characteristics (*23–26*). Elevated serum C5a levels have previously been found to correlate with clinical severity (*27*). Conversely, another study found a negative correlation with C3 and disease severity, proposed to be due to increased complement consumption (*24*). We did not see a difference in complement proteins between EOMG and LOMG, in contrast to a previous study that reported lower C3 and C4 levels in EOMG (*24*). Given the known heterogeneity of complement activation by AChR-Abs (*55*), prospective study of these complement markers prior to complement inhibitor therapies would allow assessment of their validity in predicting outcome for that targeted treatment.

There have been no previous studies exploring expression of complement receptors on lymphocytes in MG. We demonstrated higher intensity of expression of complement receptors 1 (CD35) and 2 (CD21) on B cells, despite reduced frequencies of $CD35^+$ B cells in disease, which may result in lower regulatory effects (*31*, *32*, *56*). Notably, the expression of CD55 and CD46 on T cells was also increased in MG, with the greatest difference on CD8 T cells in refractory disease. CD55 and CD46 function to inhibit the complement cascade, but ligation also has functional effects on T cells (*37*). CD55 ligation on T cells reduces IFN-γ and IL-2 production, and increases IL-10 production during antigen stimulation (*57*), as well as having regulatory effects on CD8 T cell responses (*58*). Whereas CD46 binding results initially in IFN-γ production by CD4 T cells (*59*), subsequent expansion of effector cells results in IL-2 accumulation, which then promotes Treg development (*60*). This switch to IL-10 production does not occur in CD8 T cells, and therefore the effects of CD46 on CD8 T cells are predominantly pro-inflammatory (*61*). CD46 signalling has been shown to be dysregulated in several autoimmune conditions including multiple sclerosis and rheumatoid arthritis (RA), with lack of Treg differentiation upon CD46 co-stimulation (*60*, *62*). Upregulation that is seen here is likely to be a consequence of increased complement activation by AChR-Abs, but there is a disconnect between elevated CD46 expression and Treg frequencies, suggesting that similar CD46 dysregulation may also occur in MG. Whether CD55 function in T cells in autoimmunity is also dysregulated is worthy of further study.

Previous immune profiling relating to rituximab treatment for MG focuses on B cell repopulation, rather than baseline predictive markers. Early use of rituximab is previously reported as an indication of good response (*63*), a finding we replicated here. In RA, responders to rituximab have previously demonstrated lower baseline plasmablasts compared to non-responders or healthy controls (*64*, *65*). We found that overall B cell

frequency was <3% in all non-responders (those with a less than 50% reduction in disease severity score), and >3% in those with a 50% or greater improvement. Therefore, those early in disease will respond better than those with low B cell frequencies due to longstanding immunosuppression. Additionally, rituximab non-responders displayed the highest expression of CD55 on CD8 T cells, suggesting increased complement activity in these participants; these individuals may potentially benefit from complement inhibitor therapy.

In other conditions, responders to rituximab appear to repopulate with transitional B cells, whereas poor response is associated with rapid repopulation with memory B cells (*66*). In this study, few cases repopulated, in part due to ongoing treatment for some. Following rituximab, the residual B cell population contained a high proportion of plasmablasts, likely because B cells lose CD20 expression as they differentiate into plasmablasts and plasma cells. The remaining non-depleted B cells were of a different phenotype, with low BAFF-R, CD21 and CD35 expression. BAFF-R expression has been shown to be reduced on CD19 cells following rituximab previously (*67*). Importantly, Tregs are known to expand following rituximab (*47*), a finding corroborated in this study.

Finally, in the treatment naïve cohort, those who started corticosteroid therapy were found to have the highest frequency of B cells expressing CD27, Blimp-1 and IgG, and lowest frequency of Tregs at 6-month follow-up, compared to those who didn't. Whilst these changes in B cells have been reported previously with corticosteroid treatment (*68*, *69*), Tregs are normally seen to expand (*70*, *71*). Additionally, the individual with ongoing high disease score at 6-months demonstrated an increase in Treg frequency and had the highest level of Tregs at follow-up. This highlights that other pathological mechanisms are likely at play, that may not be counteracted by Treg expansion. Interestingly, recent work has shown that the beneficial therapeutic effects of glucocorticoids are reliant upon the presence of Tregs (*71*), therefore

resistance to corticosteroids may in part be due to low Treg frequencies, although this remains unproven. Of note, our analysis of steroid effects had a small numbers of participants, and therefore further work is required to better understand its relevance.

The limitations of this study reflect those of many studies of MG. The wide heterogeneity of this rare disease makes it difficult to recruit to very specific cohorts, whilst trying to extrapolate the findings to a wider population. Here we attempted to limit this heterogeneity by only including those with AChR-positive MG, with no thymoma or other autoimmune disease that might require immunosuppression. Additionally, as a cohort study, it remains unknown whether the changes seen within the refractory cohort have evolved over time or are present at disease onset to predict outcome. Prospective recruitment of those with severe disease prior to initiation of immunotherapy is challenging, nevertheless, these findings may constitute the basis for future studies, to validate these findings as predictive biomarkers.

The immune changes shown here demonstrate alternative avenues of therapy that may be beneficial in MG. Current practice of CD20 depletion in AChR-MG is known to have variable outcomes and sometimes limited benefit, and here we illustrate the known concerns of this approach; highly differentiated B cells that produce autoantibodies are not targeted as they do not express CD20. Therefore, therapies that target plasma cells, such as anti-CD38 or BCMA in the form of monoclonal antibodies or cellular therapy are likely to have greater success, with trial results eagerly anticipated (*72*, *73*). Additionally, targeting a wider range of B cells with anti-CD19 therapy is also under evaluation in MG (*74*, *75*). Whether this translates to greater clinical efficacy, alongside an acceptable safety profile, remains to be seen.

The findings here also suggest that targeting Treg expansion could be beneficial in those with refractory MG. Promoting immune tolerance confers lower risk than widespread immunosuppression. This can be done in a number of ways involving promoting regulatory

innate immune cells (*76*, *77*), possibly via vitamin D supplementation (*78*), or adoptive transfer of Tregs which has shown therapeutic benefit in the mouse model of MG (*79–81*). Antigen-specific tolerance is likely to be more beneficial in many autoimmune diseases, as the effects are limited to the known pathology, and could represent a long-lasting "cure" to autoimmune diseases (*82*). Therapies promoting antigen-specific tolerance in AChR-MG have been investigated in MG including antigen-specific tolerogenic-DCs, antigen presenting cell-like nanoparticles, and vaccines (*82–87*). However, there are multiple disease-associated AChR-Ab epitopes (*88*), which may be why the antibody titre does not correlate well with disease severity, and suggests that antigen-specific therapies would need to be tailored to the individual.

In summary, significant alterations to the innate and adaptive immune systems are observed in AChR-MG, particularly in refractory disease. Frequency of memory B cells or Tregs, or circulating C3, C5 or clusterin levels are potential prognostic markers that are worth further prospective evaluation. Our work suggests that future treatment strategies directed at plasma cells or at promoting immune tolerance mechanisms are likely to be beneficial in refractory disease.

MATERIALS AND METHODS

Ethics

This study was approved by Health Research Authority and Health Care Research Wales and NHS Research Ethics Committee (21/NW/0188). Written informed consent was obtained for all enrolled participants.

Study Design

Participants were recruited from the Northern Care Alliance NHS Foundation Trust, the Walton Centre NHS Foundation Trust, Newcastle Hospitals NHS foundation Trust, Oxford, University College London NHS Foundation Trust, and Imperial NHS foundation Trust. Case Record Forms and clinical assessment were completed by the neurology clinical research fellow with each participant at baseline and follow-up. All participants were able to give valid consent and were aged 18 to 80 (full list available in supplementary table 1). The following inclusion criteria applied to each cohort.

Stable Immunosuppressed:

- Have a diagnosis of AChR positive myasthenia gravis (can be ocular, bulbar or generalised)
- MGFA Post-intervention Status MM or better with no clinical relapse for 2 years
- On either azathioprine or MMF along with ≤5mg/day of prednisolone
- No prednisolone dose increase or decrease in past 12 months
- No increase in azathioprine or MMF dose for 2 years (allowing for cessation for up to 1 month)

Stable Non-Immunosuppressed:

- have a diagnosis of AChR positive myasthenia gravis (can be ocular, bulbar or generalised).
- MGFA Post-intervention Status MM or better on only low-dose cholinesterase inhibitors (≤120 mg pyridostigmine/day on average) for over two years.

Refractory:

- have a diagnosis of AChR positive myasthenia gravis (can be ocular, bulbar or generalised).
- have been deemed eligible to be refractory to standard treatment and eligible for rituximab as per the NHS England criteria (England 2018).

Treatment Naïve:

- Have a diagnosis of AChR positive myasthenia gravis
- Diagnosed in previous 6 months
- Not yet taken any form of immunosuppression

Healthy Controls:

- No diagnosis of myasthenia gravis or other autoimmune condition that responds to standard immunosuppressive therapy (e.g. RA, inflammatory bowel disease).

Exclusion criteria for all cohorts included co-existing autoimmune condition for which azathioprine or mycophenolate mofetil are treatments (e.g. inflammatory bowel disease, RA, neuromyotonia), currently undergoing treatment for solid organ or haematological malignancy, or previous thymoma, or a clinical frailty scale ≥6.

Sample Processing

Whole blood was collected in two EDTA tubes and processed within 12 hours of collection. Plasma was isolated from one tube via centrifugation of whole blood at 2000g for 10 minutes at room temperature. PBMCs were isolated from a separate tube using SepMate tubes (StemCell #85460), and Ficoll-Paque Plus (GE Healthcare # GE17-1440-03) via density gradient centrifugation (1200g for 10 minutes at room temp). Cells were washed twice in FACS buffer (PBS w/o Ca^{2+}/Mg^{2+}, 2%v/v FCS, 5 mM EDTA) prior to counting, using typtan blue and a countess II automated cell counter (Thermo Fisher Scientific). PBMCs were stored in FCS with 10% DMSO at -80°C for up to 2 weeks and then transferred to liquid nitrogen or -150°C storage.

Flow Cytometry

Samples were thawed by warming at 37°C for 30 seconds then rapidly mixing with 10ml warmed complete media. Cells were washed in PBS then stained with Zombie UV™ (Biolegend, London UK) 1/500 for 15 minutes in PBS. Non-specific binding was blocked using Human FcR Blocking Reagent (Miltenyi, Bisley, UK) at 1/50 for 15 minutes. Extracellular antibodies were added at 1/50 for 30 minutes. Antibody information is provided in supplementary table 2 Cells were then fixed and permeabilised using FOXP3/Transcription Factor Staining Buffer Set (Thermo Fisher, Altrincham, UK), washed in perm buffer and stained with intracellular markers at 1:100 overnight. Cells were acquired on the LSRFortessa (BD Biosciences, Swindon, UK) and data analysed using FlowJo (v10.0; BD Biosciences). If under 50,000 lymphocytes were acquired then results were excluded from analysis.

Cell stimulation

Thawed cells were stimulated with either CD40L (R&D Systems, Abbingdon, UK) 0.5µg/ml CpGB (Cambridge Bioscience, Cambridge, UK) 1uM, or R848 (Resiquimod, InvivoGen Toulouse, France) 1µg/ml for 48 hours followed by 2µL/ml of stimulation cocktail (Thermo Fisher) in the presence of Brefeldin A (Biolegend) in the last four hours, then washed and stained for flow cytometric analysis.

Complement Immunoassays

Fifteen complement analytes were selected based on previous research showing changes in serum levels of complement biomarkers in patients with MG and the accessibility of in house enzyme linked immunosorbent assays (ELISA) (*89–92*), The marker set was selected to interrogate the classical (C1q, C3, C4), alternative (Properdin, Ba, iC3b, FH, FHR125, FHR4, FI, sCR1), and terminal (C5, C9, clusterin, TCC (terminal complement complex)) pathways. Details of the antibodies, protein standards, and assay conditions can be found in Table S2. Plasma samples stored at -80°C were thawed just before assaying, briefly vortexed, and then diluted in phosphate-buffered saline containing 0.1% Tween 20 (PBST, Sigma-Aldrich) and 0.2% bovine serum albumin (BSA) or non-fat milk (NFM; properdin assay only). Capture antibodies were fixed onto 96-well immunoplates (Thermo Fisher) overnight at 4°C, with concentrations ranging from 2–20 µg/ml in 50 µl/well of carbonate-bicarbonate buffer (pH 9.6). Wells were blocked with 2% BSA or NFM in PBST (100 µl/ well) and incubated for 1 h at 37°C, washed once with PBST, and plasma samples or protein standards diluted in buffer (0.2% BSA or NFM PBST (50 µl/ well) added in duplicate at a suitable dilution (Table S1). Plates were incubated for 1h at RT or 37°C, washed three times and detection antibodies added at appropriate concentration (1–5 µg/ml) in 50 µl/well 0.2% BSA or NFM in PBST for 1h at RT or 37°C. In assays where the detection antibody was not directly labelled, an HRP-labelled secondary

antibody (anti-mouse or anti-rabbit IgG, as applicable, Jackson ImmunoResearch, West Grove, USA) or for biotinylated antibodies, Streptavidin-HRP (R&D Systems) was used. Finally, plates were washed and developed using O-phenylenediamine dihydrochloride (OPD) substrate (Sigma-Aldrich) for 3–15 min, followed by adding 50 µl/well 5% H_2SO_4 to quench the reaction. Absorbances were read at 492 nm using Infinite F50 microplate reader (Tecan, Reading, UK). Intra- and inter-assay coefficient of variation were below 10% for all assays.

Statistical Analysis

Statistical analysis was undertaken using GraphPad PRISM (version 10.0). All data underwent normality testing. Comparison between disease and Control was with student's t-test (parametric data) or Mann-Whitney (non-parametric). Comparison between cohorts was with one-way ANOVA with Tukey multiple comparison test (parametric) or Kruskal-Wallis with Dunn's multiple comparison test (non-parametric). Results are presented as individual data points with medians. For correlation Pearson's correlation (for parametric) or Spearman's rank correlation coefficient test (for non-parametric data). In all cases, a p value of ≤ 0.05 was considered significant. Where no statistical difference is shown there was no significant difference. Details of statistical tests and definitions of n can be found in each figure legend.

Supplementary Materials:

Supplementary Fig. S1. Additional B cell subset changes seen in AChR-MG.

Supplementary Fig. S2. PD-L1, Ki-67 and BAFF-R expression on B cells, and B cell stimulation.

Supplementary Fig. S3. Additional T cell subset changes seen in AChR-MG.

Supplementary Fig. S4. Additional myeloid cell changes seen in AChR MG.

Supplementary Fig. S5. NK cell subtyping, and CD80 and CD86 expression on myeloid cells in AChR-MG.

Supplementary Fig. S6. Complement proteins in AChR-MG.

Supplementary Fig. S7. Lymphocyte complement receptor expression in AChR-MG.

Supplementary Fig. S8. Prospective changes seen following rituximab for refractory AChR-MG.

Supplementary Fig. S9. Prospective six-month follow-up of treatment naïve AChR-MG.

Supplementary Table S1. Antibodies used in flow cytometry staining

Supplementary Table S2. Antibodies, standards and sample dilutions used in complement ELISA

References and Notes:

1. N. M. Engel-Nitz, A. Boscoe, R. Wolbeck, J. Johnson, N. J. Silvestri, Burden of illness in patients with treatment refractory myasthenia gravis. *Muscle Nerve*, doi: 10.1002/mus.26114 (2018).
2. L. Harris, S. Graham, S. MacLachlan, A. Exuzides, S. Jacob, Healthcare resource utilization by patients with treatment-refractory myasthenia gravis in England. *J. Med. Econ.* **22**, 691–697 (2019).
3. J. M. Lindstrom, M. E. Seybold, V. A. Lennon, S. Whittingham, D. D. Duane, Antibody to acetylcholine receptor in myasthenia gravis. Prevalence, clinical correlates, and diagnostic value. *Neurology* **26**, 1054–1059 (1976).
4. G. I. Wolfe, J. E. Hanson, N. J. Silvestri, Myasthenia gravis: The evolving therapeutic landscape. *eNeurologicalSci* **37**, 100541 (2024).
5. C. Luo, Y. Li, W. Liu, H. Feng, H. Wang, X. Huang, L. Qiu, J. Ouyang, Expansion of circulating counterparts of follicular helper T cells in patients with myasthenia gravis. *J. Neuroimmunol.* **256**, 55–61 (2013).
6. S. Ashida, H. Ochi, M. Hamatani, C. Fujii, K. Kimura, Y. Okada, Y. Hashi, K. Kawamura, H. Ueno, R. Takahashi, T. Mizuno, T. Kondo, Immune Skew of Circulating Follicular Helper T Cells Associates With Myasthenia Gravis Severity. *Neurol Neuroimmunol Neuroinflamm* **8** (2021).
7. M. Thiruppathi, J. Rowin, Q. Li Jiang, J. R. Sheng, B. S. Prabhakar, M. N. Meriggioli, Functional defect in regulatory T cells in myasthenia gravis. *Ann. N. Y. Acad. Sci.* **1274**, 68–76 (2012).

8. A. Balandina, S. Lécart, P. Dartevelle, A. Saoudi, S. Berrih-Aknin, Functional defect of regulatory CD4+ CD25+ T cells in the thymus of patients with autoimmune myasthenia gravis. *Blood* **105**, 735–741 (2005).

9. S. Kohler, T. O. P. Keil, M. Swierzy, S. Hoffmann, H. Schaffert, M. Ismail, J. C. Rückert, T. Alexander, F. Hiepe, C. Gross, A. Thiel, A. Meisel, Disturbed B cell subpopulations and increased plasma cells in myasthenia gravis patients. *J. Neuroimmunol.* **264**, 114–119 (2013).

10. Y. Zhang, X. Jia, Y. Xia, H. Li, F. Chen, J. Zhu, X. Zhang, Y. Zhang, Y. Wang, Y. Xu, M. Pan, X. Huang, T. Yu, L. Fu, C. Xiao, D. Geng, Altered expression of transcription factors IRF4 and IRF8 in peripheral blood B cells is associated with clinical severity and circulating plasma cells frequency in patients with myasthenia gravis. *Autoimmunity* **51**, 126–134 (2018).

11. R. Fan, W. Que, Z. Liu, W. Zheng, X. Guo, L. Liu, F. Xiao, Single-cell mapping reveals dysregulation of immune cell populations and VISTA+ monocytes in myasthenia gravis. *Clin. Immunol.* **245**, 109184 (2022).

12. Z. Zhu, W. You, Z. Xie, P. Wang, Z. Liu, C. Wang, J. Bi, Mycophenolate mofetil improves neurological function and alters blood T-lymphocyte subsets in rats with experimental autoimmune encephalomyelitis. *J. Int. Med. Res.* **42**, 530–541 (2014).

13. D. Makarious, K. Horwood, J. I. G. Coward, Myasthenia gravis: An emerging toxicity of immune checkpoint inhibitors. *Eur. J. Cancer* **82**, 128–136 (2017).

14. K. Iwasa, H. Yoshikawa, Y. Furukawa, M. Yamada, Programmed cell death ligand 1 expression is upregulated in the skeletal muscle of patients with myasthenia gravis. *J. Neuroimmunol.* **325**, 74–78 (2018).

15. E. K. Bagir, A. Acikalin, A. Avci, D. Gumurdulu, S. Paydas, PD-1 and PD-L1 expression in thymic epithelial tumours and non-neoplastic thymus. *J. Clin. Pathol.* **71**, 637–641 (2018).

16. Y. Chen, Y. Zhang, X. Chai, J. Gao, G. Chen, W. Zhang, Y. Zhang, Correlation between the Expression of PD-L1 and Clinicopathological Features in Patients with Thymic Epithelial Tumors. *Biomed Res. Int.* **2018**, 5830547 (2018).
17. A. L. Corey, D. P. Richman, C. A. Shuman, C. M. Gomez, Use of monoclonal antiacetylcholine receptor antibodies to investigate the macrophage inflammation of acute experimental myasthenia gravis: refractoriness to a …. *Neurology* (1985).
18. K. Utsugisawa, Y. Nagane, S. Suzuki, R. Kondoh, Antigen-specific T-cell activation in hyperplastic thymus in myasthenia gravis. *Muscle Nerve* **36**, 100–103 (2007).
19. Y. Nagane, K. Utsugisawa, D. Obara, M. Yamagata, H. Tohgi, Dendritic cells in hyperplastic thymuses from patients with myasthenia gravis. *Muscle Nerve* **27**, 582–589 (2003).
20. Y. Song, C. Xing, T. Lu, C. Liu, W. Wang, S. Wang, X. Feng, J. Bi, Q. Wang, C. Lai, Aberrant dendritic cell subsets in patients with myasthenia gravis and related clinical features. *Neuroimmunomodulation* **30**, 69–80 (2023).
21. J. Dong, R.-S. Duan, P. Zhang, Causal relationship between the immune phenotype of monocytes and myasthenia gravis: A Mendelian randomization study. *Heliyon* **10**, e26741 (2024).
22. S. Nakano, A. G. Engel, Myasthenia gravis: Quantitative immunocytochemical analysis of inflammatory cells and detection of complement membrane attack complex at the end-plate in 30 patients. [Preprint] (1993). https://doi.org/10.1212/wnl.43.6.1167.
23. F. Romi, E. K. Kristoffersen, J. A. Aarli, N. E. Gilhus, The role of complement in myasthenia gravis: serological evidence of complement consumption in vivo. *J. Neuroimmunol.* **158**, 191–194 (2005).
24. A. Liu, H. Lin, Y. Liu, X. Cao, X. Wang, Z. Li, Correlation of C3 level with severity of generalized myasthenia gravis. *Muscle Nerve* **40**, 801–808 (2009).

25. N. Iacomino, F. Vanoli, R. Frangiamore, M. Ballardini, L. Scandiffio, F. Bortone, F. Andreetta, F. Baggi, P. Bernasconi, C. Antozzi, P. Cavalcante, R. Mantegazza, Complement activation profile in myasthenia gravis patients: Perspectives for tailoring anti-complement therapy. *Biomedicines* **10**, 1360 (2022).

26. F. Aguirre, A. Manin, V. C. Fernandez, M. E. Justo, J. Leoni, M. L. Paz, A. M. Villa, C3, C5a and anti-acetylcholine receptor antibody as severity biomarkers in myasthenia gravis. *Ther. Adv. Neurol. Disord.* **13**, 1756286420935697 (2020).

27. E. Tüzün, B. G. Scott, E. Goluszko, S. Higgs, P. Christadoss, Genetic evidence for involvement of classical complement pathway in induction of experimental autoimmune myasthenia gravis. *J. Immunol.* **171**, 3847–3854 (2003).

28. M. C. Carroll, The role of complement in B cell activation and tolerance. *Adv. Immunol.* **74**, 61–88 (2000).

29. J. R. Dunkelberger, W.-C. Song, Complement and its role in innate and adaptive immune responses. *Cell Res.* **20**, 34–50 (2010).

30. W. Yin, W. Allman, S. Ouyang, Y. Li, J. Li, P. Christadoss, H. Yang, The increased expression of CD21 on AchR specified B cells in patients with myasthenia gravis. *J. Neuroimmunol.* **256**, 49–54 (2013).

31. B. Mácsik-Valent, K. Nagy, L. Fazekas, A. Erdei, Complement Receptor Type 1 (CR1, CD35), the Inhibitor of BCR-Mediated Human B Cell Activation, Differentially Regulates TLR7, and TLR9 Induced Responses. *Front. Immunol.* **10**, 1493 (2019).

32. M. Kremlitzka, B. Mácsik-Valent, A. Polgár, E. Kiss, G. Poór, A. Erdei, Complement Receptor Type 1 Suppresses Human B Cell Functions in SLE Patients. *J Immunol Res* **2016**, 5758192 (2016).

33. J. Soltys, J. A. Halperin, Q. Xuebin, DAF/CD55 and Protectin/CD59 modulate adaptive immunity and disease outcome in experimental autoimmune myasthenia gravis. *J. Neuroimmunol.* **244**, 63–69 (2012).

34. L. L. Kusner, J. A. Halperin, H. J. Kaminski, Cell surface complement regulators moderate experimental myasthenia gravis pathology. *Muscle Nerve* **47**, 33–40 (2013).

35. M. Capasso, L. G. Durrant, M. Stacey, S. Gordon, J. Ramage, I. Spendlove, Costimulation via CD55 on human CD4+ T cells mediated by CD97. *J. Immunol.* **177**, 1070–1077 (2006).

36. M. P. Longhi, C. L. Harris, B. P. Morgan, A. Gallimore, Holding T cells in check--a new role for complement regulators? *Trends Immunol.* **27**, 102–108 (2006).

37. N. H. S. England, Rituximab biosimilar for the treatment of myasthenia gravis in adults. Version 2. (2021).

38. A. E. Renton, H. A. Pliner, C. Provenzano, A. Evoli, R. Ricciardi, M. A. Nalls, G. Marangi, Y. Abramzon, S. Arepalli, S. Chong, D. G. Hernandez, J. O. Johnson, E. Bartoccioni, F. Scuderi, M. Maestri, J. R. Gibbs, E. Errichiello, A. Chiò, G. Restagno, M. Sabatelli, M. Macek, S. W. Scholz, A. Corse, V. Chaudhry, M. Benatar, R. J. Barohn, A. McVey, M. Pasnoor, M. M. Dimachkie, J. Rowin, J. Kissel, M. Freimer, H. J. Kaminski, D. B. Sanders, B. Lipscomb, J. M. Massey, M. Chopra, J. F. Howard Jr, W. J. Koopman, M. W. Nicolle, R. M. Pascuzzi, A. Pestronk, C. Wulf, J. Florence, D. Blackmore, A. Soloway, Z. Siddiqi, S. Muppidi, G. Wolfe, D. Richman, M. M. Mezei, T. Jiwa, J. Oger, D. B. Drachman, B. J. Traynor, A genome-wide association study of myasthenia gravis. *JAMA Neurol.* **72**, 396–404 (2015).

39. L. Sun, Y. Meng, Y. Xie, H. Zhang, Z. Zhang, X. Wang, B. Jiang, W. Li, Y. Li, Z. Yang, CTLA4 variants and haplotype contribute genetic susceptibility to myasthenia gravis in northern Chinese population. *PLoS One* **9**, e101986 (2014).

40. X. B. Wang, R. Pirskanen, R. Giscombe, A. K. Lefvert, Two SNPs in the promoter region of the CTLA-4 gene affect binding of transcription factors and are associated with human myasthenia gravis. [Preprint] (2007). https://doi.org/10.1111/j.1365-2796.2007.01879.x.
41. M. L. Fichtner, R. Jiang, A. Bourke, R. J. Nowak, K. C. O'Connor, Autoimmune Pathology in Myasthenia Gravis Disease Subtypes Is Governed by Divergent Mechanisms of Immunopathology. *Front. Immunol.* **11**, 776 (2020).
42. G. Dorcet, H. Migné, D. Biotti, C. Bost, F. Lerebours, J. Ciron, E. Treiner, Early B cells repopulation in multiple sclerosis patients treated with rituximab is not predictive of a risk of relapse or clinical progression. *J. Neurol.* **269**, 5443–5453 (2022).
43. Y. Hu, J. Wang, J. Rao, X. Xu, Y. Cheng, L. Yan, Y. Wu, N. Wu, X. Wu, Comparison of peripheral blood B cell subset ratios and B cell-related cytokine levels between ocular and generalized myasthenia gravis. *Int. Immunopharmacol.* **80**, 106130 (2020).
44. M. E. Hill, H. Shiono, J. Newsom-Davis, N. Willcox, The myasthenia gravis thymus: a rare source of human autoantibody-secreting plasma cells for testing potential therapeutics. *J. Neuroimmunol.* **201–202**, 50–56 (2008).
45. T. Hirano, IL-6 in inflammation, autoimmunity and cancer. *Int. Immunol.* **33**, 127–148 (2021).
46. P. Wang, S. G. Zheng, Regulatory T cells and B cells: implication on autoimmune diseases. *Int. J. Clin. Exp. Pathol.* **6**, 2668–2674 (2013).
47. S. Jing, J. Lu, J. Song, S. Luo, L. Zhou, C. Quan, J. Xi, C. Zhao, Effect of low-dose rituximab treatment on T- and B-cell lymphocyte imbalance in refractory myasthenia gravis. [Preprint] (2019). https://doi.org/10.1016/j.jneuroim.2019.05.004.

48. C. Ngo, C. Garrec, E. Tomasello, M. Dalod, The role of plasmacytoid dendritic cells (pDCs) in immunity during viral infections and beyond. *Cell. Mol. Immunol.* **21**, 1008–1035 (2024).

49. P. Chen, Y. Li, H. Huang, Y. Li, X. Huang, Z. Chen, X. Liu, L. Qiu, C. Ou, Z. Huang, Z. Lin, H. Ran, W. Liu, Imbalance of the two main circulating dendritic cell subsets in patients with myasthenia gravis. *Clin. Immunol.* **205**, 130–137 (2019).

50. A. Melms, G. Malcherek, U. Gern, N. Sommer, R. Weissert, H. Wiethölter, H. J. Bühring, Thymectomy and azathioprine have no effect on the phenotype of CD4 T lymphocyte subsets in myasthenia gravis. *J. Neurol. Neurosurg. Psychiatry* **56**, 46–51 (1993).

51. C. G. Mueller, C. Boix, W.-H. Kwan, C. Daussy, E. Fournier, W. H. Fridman, T. J. Molina, Critical role of monocytes to support normal B cell and diffuse large B cell lymphoma survival and proliferation. *J. Leukoc. Biol.* **82**, 567–575 (2007).

52. Y. Zheng, C. N. Manzotti, M. Liu, F. Burke, K. I. Mead, D. M. Sansom, CD86 and CD80 differentially modulate the suppressive function of human regulatory T cells. *J. Immunol.* **172**, 2778–2784 (2004).

53. X.-Y. Lai, M.-C. Gui, J. Lin, Y. Li, X. Luo, L.-X. Li, B.-T. Bu, Peripheral NK and B regulatory cell frequencies are altered with symptomatic exacerbation in generalized myasthenia gravis patients. (2017).

54. S. S. Yandamuri, B. Filipek, N. Lele, I. Cohen, J. L. Bennett, R. J. Nowak, E. S. Sotirchos, E. E. Longbrake, E. M. Mace, K. C. O'Connor, A Noncanonical CD56dimCD16dim/- NK Cell Subset Indicative of Prior Cytotoxic Activity Is Elevated in Patients with Autoantibody-Mediated Neurologic Diseases. *J. Immunol.*, doi: 10.4049/jimmunol.2300015 (2024).

55. A. H. Obaid, C. Zografou, D. D. Vadysirisack, B. Munro-Sheldon, M. L. Fichtner, B. Roy, W. M. Philbrick, J. L. Bennett, R. J. Nowak, K. C. O'Connor, Heterogeneity of acetylcholine

receptor autoantibody–mediated complement activity in patients with myasthenia gravis. *Neurol. Neuroimmunol. Neuroinflamm.* **9**, e1169 (2022).

56. M. Kremlitzka, A. Polgár, L. Fülöp, E. Kiss, G. Poór, A. Erdei, Complement receptor type 1 (CR1, CD35) is a potent inhibitor of B-cell functions in rheumatoid arthritis patients. *Int. Immunol.* **25**, 25–33 (2013).
57. J. Liu, T. Miwa, B. Hilliard, Y. Chen, J. D. Lambris, A. D. Wells, W.-C. Song, The complement inhibitory protein DAF (CD55) suppresses T cell immunity in vivo. *J. Exp. Med.* **201**, 567–577 (2005).
58. C. Fang, T. Miwa, H. Shen, W.-C. Song, Complement-dependent enhancement of CD8+ T cell immunity to lymphocytic choriomeningitis virus infection in decay-accelerating factor-deficient mice. *J. Immunol.* **179**, 3178–3186 (2007).
59. A. Sánchez, M. J. Feito, J. M. Rojo, CD46-mediated costimulation induces a Th1-biased response and enhances early TCR/CD3 signaling in human CD4+ T lymphocytes. *Eur. J. Immunol.* **34**, 2439–2448 (2004).
60. J. Cardone, G. Le Friec, P. Vantourout, A. Roberts, A. Fuchs, I. Jackson, T. Suddason, G. Lord, J. P. Atkinson, A. Cope, A. Hayday, C. Kemper, Complement regulator CD46 temporally regulates cytokine production by conventional and unconventional T cells. *Nat. Immunol.* **11**, 862–871 (2010).
61. A. S. Hansen, J. Slater, M. Biltoft, B. B. Bundgaard, B. K. Møller, P. Höllsberg, CD46 is a potent co-stimulatory receptor for expansion of human IFN-γ-producing CD8 + T cells. *Immunol. Lett.* **200**, 26–32 (2018).
62. A. L. Astier, G. Meiffren, S. Freeman, D. A. Hafler, Alterations in CD46-mediated Tr1 regulatory T cells in patients with multiple sclerosis. *J. Clin. Invest.* **116**, 3252–3257 (2006).

63. S. Brauner, A. Eriksson-Dufva, M. A. Hietala, T. Frisell, Rayomand Press, F. Piehl, Comparison between rituximab treatment for new-onset generalized myasthenia gravis and refractory generalized myasthenia gravis. *JAMA Neurol.* **77**, 974 (2020).

64. H.-P. Brezinschek, F. Rainer, K. Brickmann, W. B. Graninger, B lymphocyte-typing for prediction of clinical response to rituximab. *Arthritis Res. Ther.* **14**, R161 (2012).

65. K. Owczarczyk, P. Lal, A. R. Abbas, K. Wolslegel, C. T. J. Holweg, W. Dummer, A. Kelman, P. Brunetta, N. Lewin-Koh, M. Sorani, D. Leong, P. Fielder, D. Yocum, C. Ho, W. Ortmann, M. J. Townsend, T. W. Behrens, A plasmablast biomarker for nonresponse to antibody therapy to CD20 in rheumatoid arthritis. *Sci. Transl. Med.* **3**, 101ra92 (2011).

66. J. H. Anolik, B cell biology: implications for treatment of systemic lupus erythematosus. *Lupus* **22**, 342–349 (2013).

67. E. Becerra, M. A. Scully, M. J. Leandro, E. O. Heelas, J.-P. Westwood, I. De La Torre, G. Cambridge, Effect of rituximab on B cell phenotype and serum B cell-activating factor levels in patients with thrombotic thrombocytopenic purpura. *Clin. Exp. Immunol.* **179**, 414–425 (2015).

68. M. Lanzillotta, E. Della-Torre, R. Milani, E. Bozzolo, E. Bozzalla-Cassione, L. Rovati, P. G. Arcidiacono, S. Partelli, M. Falconi, F. Ciceri, L. Dagna, Increase of circulating memory B cells after glucocorticoid-induced remission identifies patients at risk of IgG4-related disease relapse. *Arthritis Res. Ther.* **20**, 222 (2018).

69. L. M. Franco, M. Gadkari, K. N. Howe, J. Sun, L. Kardava, P. Kumar, S. Kumari, Z. Hu, I. D. C. Fraser, S. Moir, J. S. Tsang, R. N. Germain, Immune regulation by glucocorticoids can be linked to cell type-dependent transcriptional responses. *J. Exp. Med.* **216**, 384–406 (2019).

70. L. Cari, F. De Rosa, G. Nocentini, C. Riccardi, Context-Dependent Effect of Glucocorticoids on the Proliferation, Differentiation, and Apoptosis of Regulatory T Cells: A Review of the Empirical Evidence and Clinical Applications. *Int. J. Mol. Sci.* **20** (2019).

71. D. Kim, Q. T. Nguyen, J. Lee, S. H. Lee, A. Janocha, S. Kim, H. T. Le, N. Dvorina, K. Weiss, M. J. Cameron, K. Asosingh, S. C. Erzurum, W. M. Baldwin 3rd, J.-S. Lee, B. Min, Anti-inflammatory Roles of Glucocorticoids Are Mediated by Foxp3+ Regulatory T Cells via a miR-342-Dependent Mechanism. *Immunity* **53**, 581-596.e5 (2020).

72. T. Chang, Safety and Efficacy of CD19-BCMA Targeted CAR-T Therapy for Refractory Generalized Myasthenia Gravis. NCT06371040, *Clinicaltrials.gov* (2024). https://www.clinicaltrials.gov/study/NCT06371040?cond=Myasthenia%20Gravis&page=1&rank=9.

73. Takeda, A Study of TAK-079 in People With Generalized Myasthenia Gravis. NCT04159805, *Clinicaltrials.gov* (2023). https://www.clinicaltrials.gov/study/NCT04159805?cond=Myasthenia%20Gravis&page=5&rank=49.

74. Amgen, Myasthenia Gravis Inebilizumab Trial (MINT). NCT04524273, *Clinicaltrials.gov* (2024). https://www.clinicaltrials.gov/study/NCT04524273?cond=Myasthenia%20Gravis&page=1&rank=8.

75. A Study of Anti-CD19 Chimeric Antigen Receptor T-Cell Therapy, in Subjects With Refractory Generalized Myasthenia Gravis. NCT06193889, *clinicaltrials.gov* (2024). https://www.clinicaltrials.gov/study/NCT06193889?cond=Myasthenia.

76. J. Liu, X. Cao, Regulatory dendritic cells in autoimmunity: A comprehensive review. *J. Autoimmun.* **63**, 1–12 (2015).

77. J. R. Sheng, L. Li, B. B. Ganesh, C. Vasu, B. S. Prabhakar, M. N. Meriggioli, Suppression of experimental autoimmune myasthenia gravis by granulocyte-macrophage colony-stimulating factor is associated with an expansion of FoxP3+ regulatory T cells. *J. Immunol.* **177**, 5296–5306 (2006).

78. H. Askmark, L. Haggård, I. Nygren, A. R. Punga, Vitamin D deficiency in patients with myasthenia gravis and improvement of fatigue after supplementation of vitamin D3: a pilot study. *Eur. J. Neurol.* **19**, 1554–1560 (2012).

79. K. M. Danikowski, S. Jayaraman, B. S. Prabhakar, Regulatory T cells in multiple sclerosis and myasthenia gravis. *J. Neuroinflammation* **14**, 117 (2017).

80. S. S. Duffy, B. A. Keating, G. Moalem-Taylor, Adoptive transfer of regulatory T cells as a promising immunotherapy for the treatment of multiple sclerosis. *Front. Neurosci.* **13** (2019).

81. M. E. Himmel, Y. Yao, P. C. Orban, T. S. Steiner, M. K. Levings, Regulatory T-cell therapy for inflammatory bowel disease: more questions than answers. *Immunology* **136**, 115–122 (2012).

82. N. Benne, D. Ter Braake, A. J. Stoppelenburg, F. Broere, Nanoparticles for Inducing Antigen-Specific T Cell Tolerance in Autoimmune Diseases. *Front. Immunol.* **13**, 864403 (2022).

83. D. T. Braake, D. ter Braake, N. Benne, C. Y. J. Lau, E. Mastrobattista, F. Broere, Retinoic Acid-Containing Liposomes for the Induction of Antigen-Specific Regulatory T Cells as a Treatment for Autoimmune Diseases. [Preprint] (2021). https://doi.org/10.3390/pharmaceutics13111949.

84. C. Keijzer, R. van der Zee, W. van Eden, F. Broere, Treg inducing adjuvants for therapeutic vaccination against chronic inflammatory diseases. *Front. Immunol.* **4**, 245 (2013).

85. P. Serra, P. Santamaria, Peptide-MHC-Based Nanomedicines for the Treatment of Autoimmunity: Engineering, Mechanisms, and Diseases. *Front. Immunol.* **11**, 621774 (2020).

86. L. Almenara-Fuentes, S. Rodriguez-Fernandez, E. Rosell-Mases, K. Kachler, A. You, M. Salvado, D. Andreev, U. Steffen, H. Bang, A. Bozec, G. Schett, R. Le Panse, J. Verdaguer, M. Dalmases, S. Rodriguez-Vidal, B. Barneda-Zahonero, M. Vives-Pi, A new platform for autoimmune diseases. Inducing tolerance with liposomes encapsulating autoantigens. *Nanomedicine* **48**, 102635 (2023).

87. Curavac, Safety, Tolerability and Immunogenic Response of CV-MG01 in Patients With Myasthenia Gravis. NCT02609022, *Clinicaltrials.gov* (2019). https://www.clinicaltrials.gov/study/NCT02609022?cond=Myasthenia%20Gravis&page=7&rank=64.

88. M. P. Protti, A. A. Manfredi, C. Straub, X. D. Wu, J. F. Howard Jr, B. M. Conti-Tronconi, Use of synthetic peptides to establish anti-human acetylcholine receptor CD4+ cell lines from myasthenia gravis patients. *J. Immunol.* **144**, 1711–1720 (1990).

89. Y. Ozawa, A. Uzawa, M. Yasuda, Y. Kojima, F. Oda, K. Himuro, N. Kawaguchi, S. Kuwabara, Changes in serum complements and their regulators in generalized myasthenia gravis. *Eur. J. Neurol.* **28**, 314–322 (2021).

90. W. L. Nastuk, O. J. Plescia, K. E. Osserman, Changes in Serum Complement Activity in Patients with Myasthenia Gravis. *Proc. Soc. Exp. Biol. Med.* **105**, 177–184 (1960).

91. E. Lekova, W. M. Zelek, D. Gower, C. Spitzfaden, I. H. Osuch, E. John-Morris, L. Stach, D. Gormley, A. Sanderson, A. Bridges, E. R. Wear, S. Petit-Frere, M. N. Burden, R. Priest, T. Wattam, S. J. Kitchen, M. Feeney, S. Davis, B. P. Morgan, E.-M. Nichols, Discovery of

functionally distinct anti-C7 monoclonal antibodies and stratification of anti-nicotinic AChR positive Myasthenia Gravis patients. *Front. Immunol.* **13**, 968206 (2022).

92. Y. Ozawa, A. Uzawa, Y. Onishi, M. Yasuda, Y. Kojima, S. Kuwabara, Activation of the classical complement pathway in myasthenia gravis with acetylcholine receptor antibodies. *Muscle Nerve* **68**, 798–804 (2023).

Acknowledgments:

We would like to acknowledge the study participants for their contribution, the University of Manchester Flow Cytometry Facility, Peter West, Holly Sedgwick, Maana Layeghi, Halima Ali-Shuwa, Rinal Sahputra, Bethany Potts, and Sara Kirkham for assistance and technical expertise and B. Paul Morgan and Tracy Hussell for intellectual input.

Funding:

This study was funded by the NorthCare Charity fund (CS2041), Myaware, and The Neuromuscular Study Group to K.D., and the AMS Springboard Award (SBF006\1165) to M.M. M.M. is also the recipient of a UKRI Future Leaders Fellowship (MR/X03383X/1).

Author Contributions

Conceptualization: KCD, JSu, MM; Methodology: KCD, KB, JKLH, MIL, JSp, SV, WMZ, JSu, MM; Investigation: KCD, KB, JKLH, MIL, JSp, SV, WMZ, JSu, MM; Visualization and Data Analysis: KCD, MM; Funding acquisition: KCD, JSu; Project administration: KCD; Supervision: JSu, MM; Writing – original draft: KCD, MM; Writing – review & editing: KCD, KB, JKLH, MIL, JSp, SV, WMZ, JSu, MM

Competing interests:

JKLH has done paid advisory boards for argenx and consultancy for Adivo Associates related to myasthenia. MIL has received speaker honoraria or travel grants from UCB Pharma and Horizon Therapeutics, and consultancy fees from UCB Pharma. She serves on scientific or educational advisory boards for UCB Pharma, Argenx and Horizon Therapeutics. JSp has received speakers fees from Argenx, UCB and J&J, travel support from Argenx and UCB and has served on advisory boards for UCB, Argenx and J&J. Stuart Viegas has received speaker honoraria or travel grants from UCB Pharma. KD, KB, WMZ, JSu and MM declare no conflicts of interest.

Data and materials availability: Data is available upon reasonable request.

Supplementary Figures

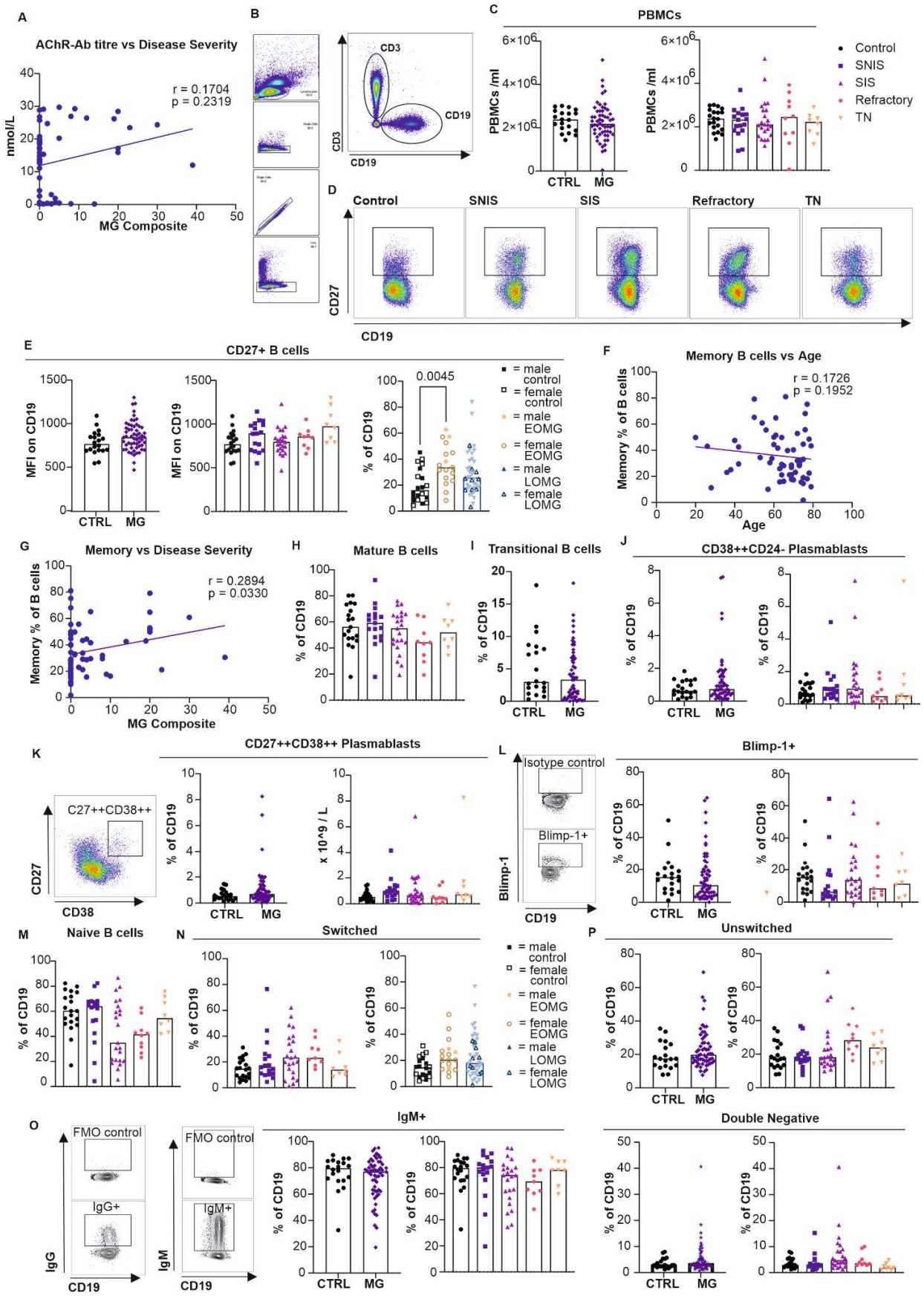

Supplementary Figure 1.

Fig S1. Additional B cell subset changes seen in AChR-MG

(A) AChR titre correlated with disease severity (n=51). **(B)** Representative FACS gating strategy for CD19 live lymphocytes in PBMCs. **(C)** Graphs showing PBMC count /ml of blood in control (n=20) compared to MG (n=58), and between subgroups; control (n-20), SNIS (n=17), SIS (n=23), refractory (n=10), and TN (n=8).**(D)** Representative FACS plots for CD27+ B cells for control, SNIS, SIS, refractory and TN cohorts. **(E)** Graphs showing CD27 MFI on B cells in control (n=20) compared to MG (n=57), between subgroups Control (n=20), SNIS (n=17), SIS (n=22), refractory (n=10), and TN (n=8), and split into early- (n=17) or late-onset MG (n=40). **(F)** Graph showing simple linear regression between memory B cell frequency and age (n=57). **(G)** Graphs showing simple linear regression between memory B cell frequency and disease severity (n=57). **(H)** Graph showing mature B cell frequency within CD19+ B cells in subgroups; control (n=20), SNIS (n=17), SIS (n=22), refractory (n=9), and TN (n=8). **(I)** Graph showing transitional B cell frequency within CD19+ B cells in Control (n=20) compared to MG (n=57). **(J)** Graphs showing CD38++CD24- plasmablast frequencies in control (n=20) compared to MG (n=57), and between subgroups; control (n-20), SNIS (n=17), SIS (n=22), refractory (n=9), and TN (n=8). **(K)** FACS plot demonstrating CD27++CD38++ gating, gated on CD19+ B cells, and graphs showing CD38++CD27++ plasmablasts frequencies in control (n=20) compared to MG (n=57), and between subgroups; control (n=20), SNIS (n=17), SIS (n=22), refractory (n=9), and TN (n=8). **(L)** FACS plots demonstrating Blimp-1 gating strategy, gated on CD19+ B cells, and graphs showing Blimp-1+ B cell frequency in control (n=20) compared to MG (n=57), and between subgroups; control (n-20), SNIS (n=17), SIS (n=22), refractory (n=10), and TN (n=8). **(M)** Graphs showing naïve (IgD+CD27-) B cells in subgroups; control (n=20), SNIS (n=17), SIS (n=22), refractory (n=9), and TN (n=8). **(N)** Graph showing switched B cell frequencies in subgroups; control (n=20), SNIS (n=17), SIS (n=22), refractory (n=9), and TN (n=8), and when split into early- (n=17) or late-onset MG (n=40). **(O)** FACS plots displaying IgG and IgM gating strategies, gated on CD19+ B cells, and graphs showing frequencies of IgM+ B cells in control (n=20) compared to MG (n=57), and between subgroups; control (n=20), SNIS (n=17), SIS (n=22), refractory (n=9), and TN (n=8). **(P)** Graphs showing unswitched memory and double negative (IgD-CD27-) B cells in control (n=20) compared to MG (n=57), and between subgroups; control (n=20) SNIS (n=17), SIS (n=22), refractory (n=9), and TN (n=8).

Graphs show individual participant data, with bar representing median values. All comparisons are performed by student's t-test or one-way ANOVA with Tukey multiple comparison test (parametric data) or Mann-Whitney or Kruskal-Wallis with Dunn's multiple comparison test (non-parametric). Correlation is calculated by Pearson (parametric) or Spearman correlation (non-parametric).

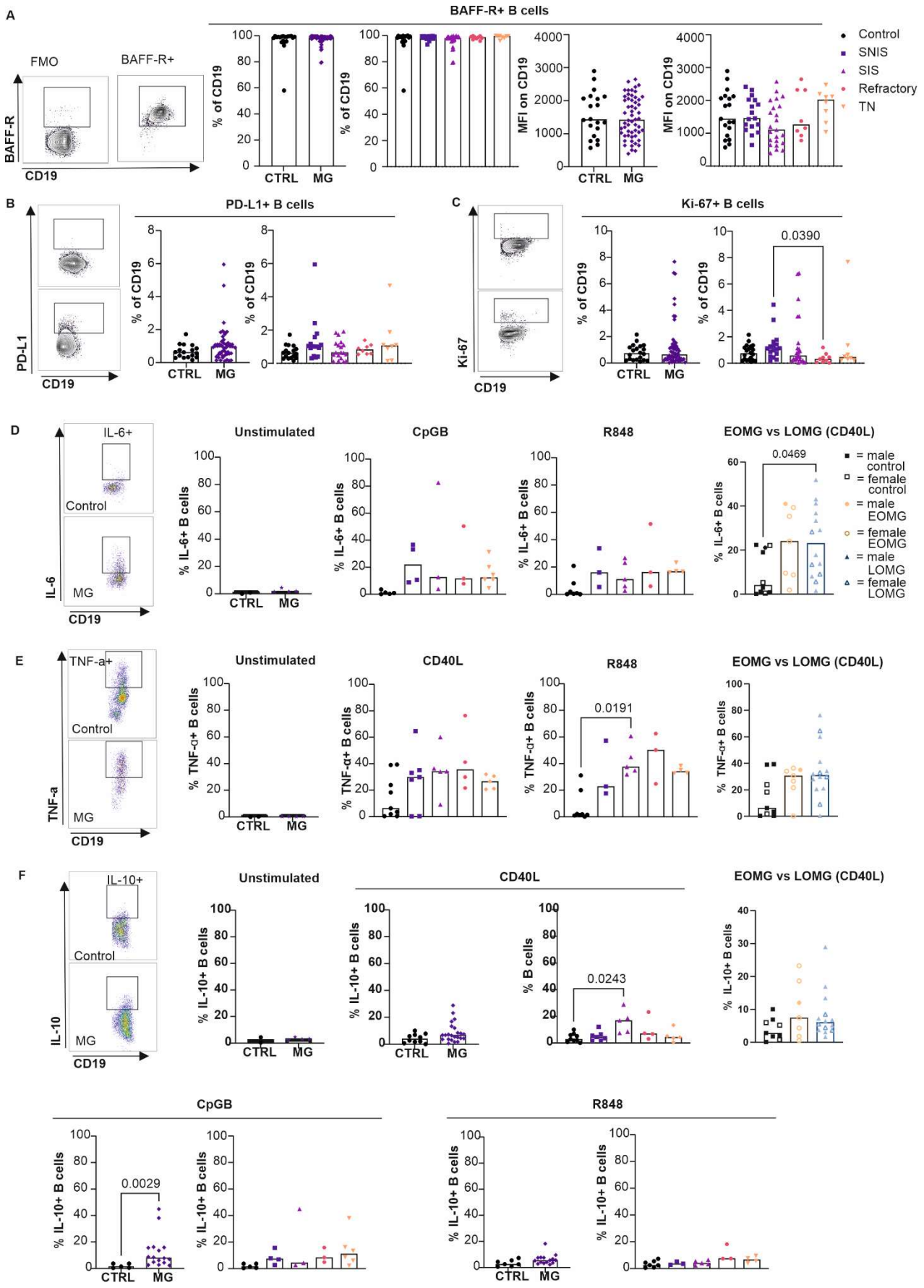

Supplementary Figure 2.

Fig S2. PD-L1, Ki-67 and BAFF-R expression on B cells, and B cell stimulation effects.

(A) FACS plot displaying BAFF-R gating strategy using an FMO, gated on CD19+ B cells, along with graphs showing frequencies and expression of BAFF-R+ B cells, in control (n=20) compared to MG (n=57), and between MG subgroups; Control (n=20), SNIS (n=17), SIS (n=22), Refractory (n=9), and TN (n=8). **(B)** FACS plot displaying PD-L1 gating strategy using an FMO, gated on CD19+ B cells, along with graphs showing frequencies of PD-L1+ B cells, in control (n=20) compared to MG (n=57), and between subgroups; control (n=20), SNIS (n=17), SIS (n=22), refractory (n=9), and TN (n=8). **(C)** FACS plot displaying Ki-67 gating strategy using an FMO, gated on CD19+ B cells, along with graphs showing frequencies of Ki-67+ B cells in control (n=20) compared to MG (n=57), and between subgroups; control (n=20), SNIS (n=17), SIS (n=22), Refractory (n=9), and TN (n=8). **(D)** Representative FACS plot demonstrating IL-6+ B cells in control compared to MG, and graphs showing IL-6 positive B cells when unstimulated in control (n=2) compared to MG (n=4), between subgroups following stimulation with CPGB and R848; control (n=5 CPGB, n=7 R848), SNIS (n=4 CPGB, n=4 R848), SIS (n=3 CPGB, n=6 R848), refractory (n=4 CPGB, n=4 R848), and TN (n=6 CPGB, n=5 R848), and frequencies of IL-6+ B cells following CD40L when split into early- (n=17) or late-onset MG (n=40). **(E)** Representative FACS plot demonstrating TNF-α+ B cells in control compared to MG, and graphs showing TNF-a positive B cells when unstimulated in control (n=2) compared to MG (n=4), between subgroups following stimulation with CD40L and R848; control (n=5 CPGB, n=7 R848), SNIS (n=4 CPGB, n=3 R848), SIS (n=3 CPGB, n=5 R848), refractory (n=4 CPGB, n=3 R848), and TN (n=6 CPGB, n=4 R848), and frequencies of TNF-a+ B cells following CD40L when split into early- (n=17) or late-onset MG (n=40). **(F)** Representative FACS plot demonstrating IL-10+ B cells in control compared to MG, and graphs showing IL-10 positive B cells following stimulation with CD40L, CPGB and R848 in control (n= 9 CD40L, n=5 CPGB, n=10 R848) compared to MG (n=21 CD40L, n=19 CPGB, n=15 R848), and between subgroups; control (n= 9 CD40L, n=5 CPGB, n=10 R848), SNIS (n=7 CD40L, n=4 CPGB, n=3 R848), SIS (n=5 CD40L, n=3 CPGB, n=5 R848), refractory (n=4 CD40L, n=4 CPGB, n=3 R848), and TN (n=5 CD40L, n=6 CPGB, n=4 R848), and frequencies of IL-10+ B cells following CD40L when split into early- (n=17) or late-onset MG (n=40)
Graphs show individual participant data, with bar representing median values. All comparisons are performed by student's t-test or one-way ANOVA with Tukey multiple

comparison test (parametric data) or Mann-Whitney or Kruskal-Wallis with Dunn's multiple comparison test (non-parametric).

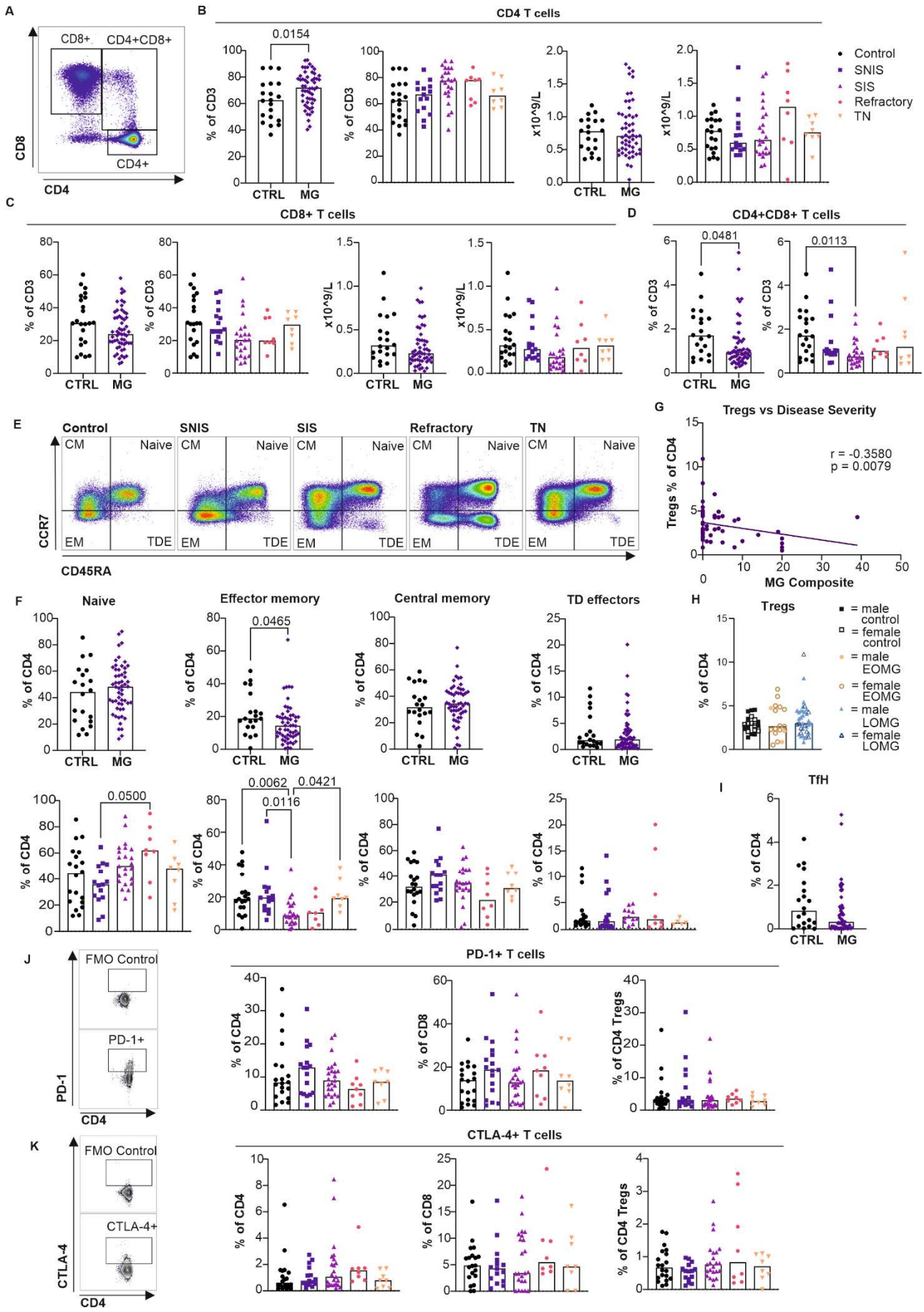

Supplementary Figure 3.

Fig. S3. Additional T cell subset changes seen in AChR-MG

(A) FACS plot showing CD4+, CD8+ and CD4+CD8+ gating, gated on CD3+ live lymphocytes in PBMCs. **(B)** Graphs showing CD4+ frequency and count in control (n=20) compared to MG (n=54), and between MG subgroups; SNIS (n=15), SIS (n=23), refractory (n=8), and TN (n=8). **(C)** Graphs showing CD8+ frequency and count in control (n=20) compared to MG (n=54), and between MG subgroups; SNIS (n=15), SIS (n=23), refractory (n=8), and TN (n=8). **(D)** Graphs showing CD4+CD8+ frequency in control (n=20) compared to MG (n=54), and between MG subgroups; SNIS (n=15), SIS (n=23), refractory (n=8), and TN (n=8). **(E)** Representative FACS plots demonstrating gating of naïve, central and effector memory and TD T cells. **(F)** Graphs showing naïve, effector and central memory and TD effector T cell frequency in control (n=20) compared to MG (n=54), as well as in subgroups; control (n=20), SNIS (n=15), SIS (n=23), refractory (n=8), and TN (n=8). **(G)** Graph showing simple linear regression for Treg frequency against disease severity (n=54) **(H)** Graph showing Treg frequencies in control (n=20), compared to EOMG (n=16) and LOMG (n=33). **(I)** Graph showing frequency of Tfh cells in control (n=20) compared to MG (n=54). **(J)** FACS plot demonstrating gating strategy for PD-1+ CD4 T cells, and graphs showing PD-1+ CD4, CD4 Treg, and CD8 T cell frequency in control (n=20), SNIS (n=15), SIS (n=23), refractory (n=8), and TN (n=8). **(K)** FACS plot demonstrating gating strategy for CTLA-4+ CD4 T cells, and graphs showing PD-1+ CD4, CD4 Treg, and CD8 T cell frequency in control (n=20), SNIS (n=15), SIS (n=23), refractory (n=8), and TN (n=8).

Graphs show individual participant data, with bar representing median values. All comparisons are performed by student's t-test or one-way ANOVA with Tukey multiple comparison test (parametric data) or Mann-Whitney or Kruskal-Wallis with Dunn's multiple comparison test (non-parametric). Correlation is calculated by Pearson (parametric) or Spearman correlation (non-parametric).

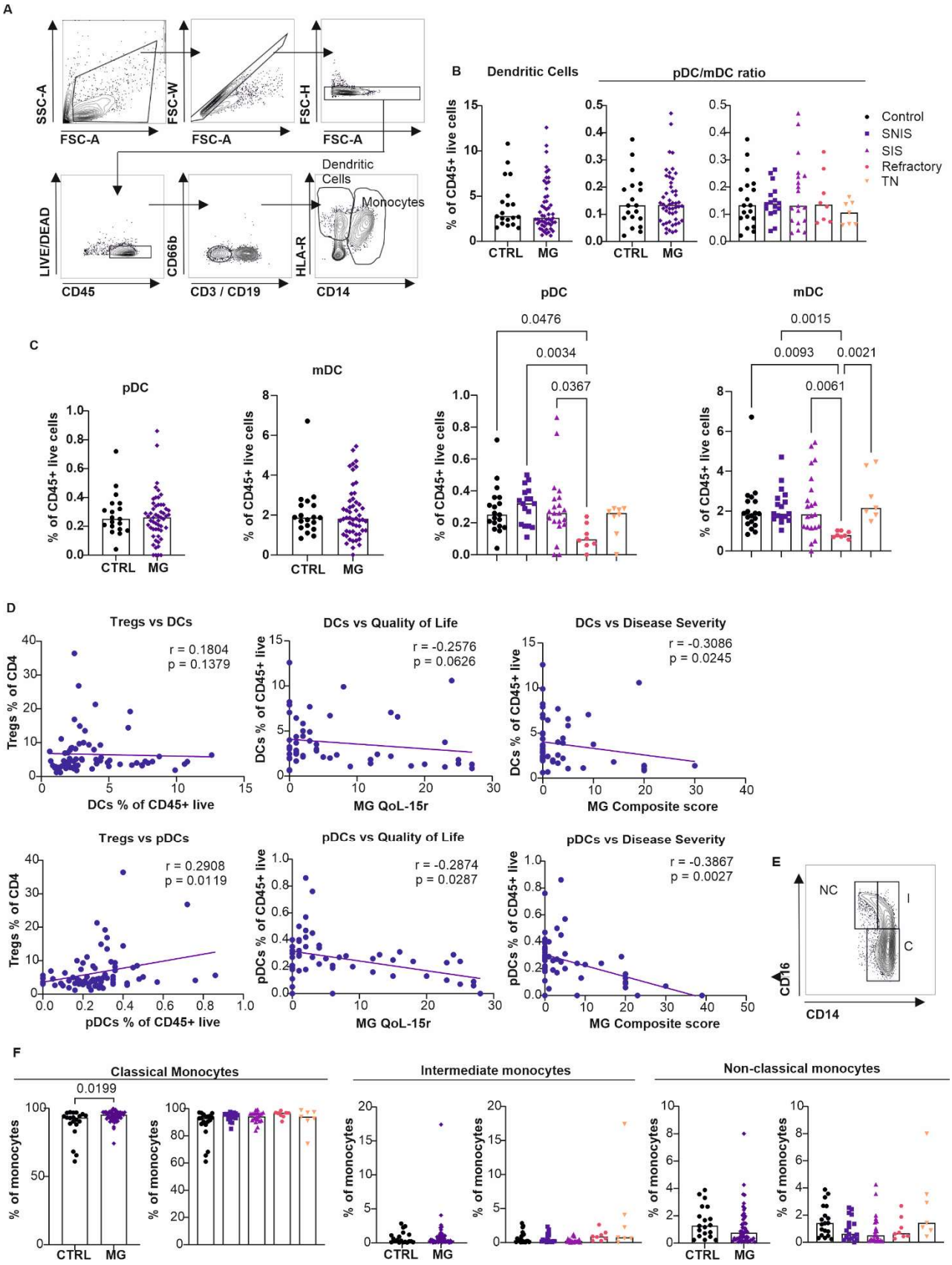

Supplementary Figure 4.

Fig. S4. Additional myeloid cell changes seen in AChR MG

(A) Representative FACS plot demonstrating gating strategy for dendritic cells and monocytes. **(B)** Graph showing DC frequency and pDC/mDC ratio in control (n=18) compared to MG (n=48), and pDC/mDC ratio in subgroups; control (n=18), SNIS (n=17), SIS (n=19), refractory (n=6), TN (n=6). **(C)** GraphS showing pDC and mDC frequency in control (n=18) compared to MG (n=48), and in subgroups; control (n=18), SNIS (n=17), SIS (n=19), refractory (n=6), TN (n=6). **(D)** Graphs showing simple linear regression for DCs and pDCs vs and Treg frequency (n=74), quality of life (n=53), and disease severity (n=53). **(E)** Representative FACS plot demonstrating gating strategy for classical (C), intermediate (I) and non-classical (NC) monocytes. **(F)** Graphs showing frequencies of classical, intermediate and non-classical monocytes in control (n=18), compared to MG (n=48), and in subgroups control (n=18), SNIS (n=17), SIS (n=19), refractory (n=6), and TN (n=6).

Graphs show individual participant data, with bar representing median values. All comparisons are performed by student's t-test or one-way ANOVA with Tukey multiple comparison test (parametric data) or Mann-Whitney or Kruskal-Wallis with Dunn's multiple comparison test (non-parametric). Correlation is calculated by Pearson (parametric) or Spearman correlation (non-parametric).

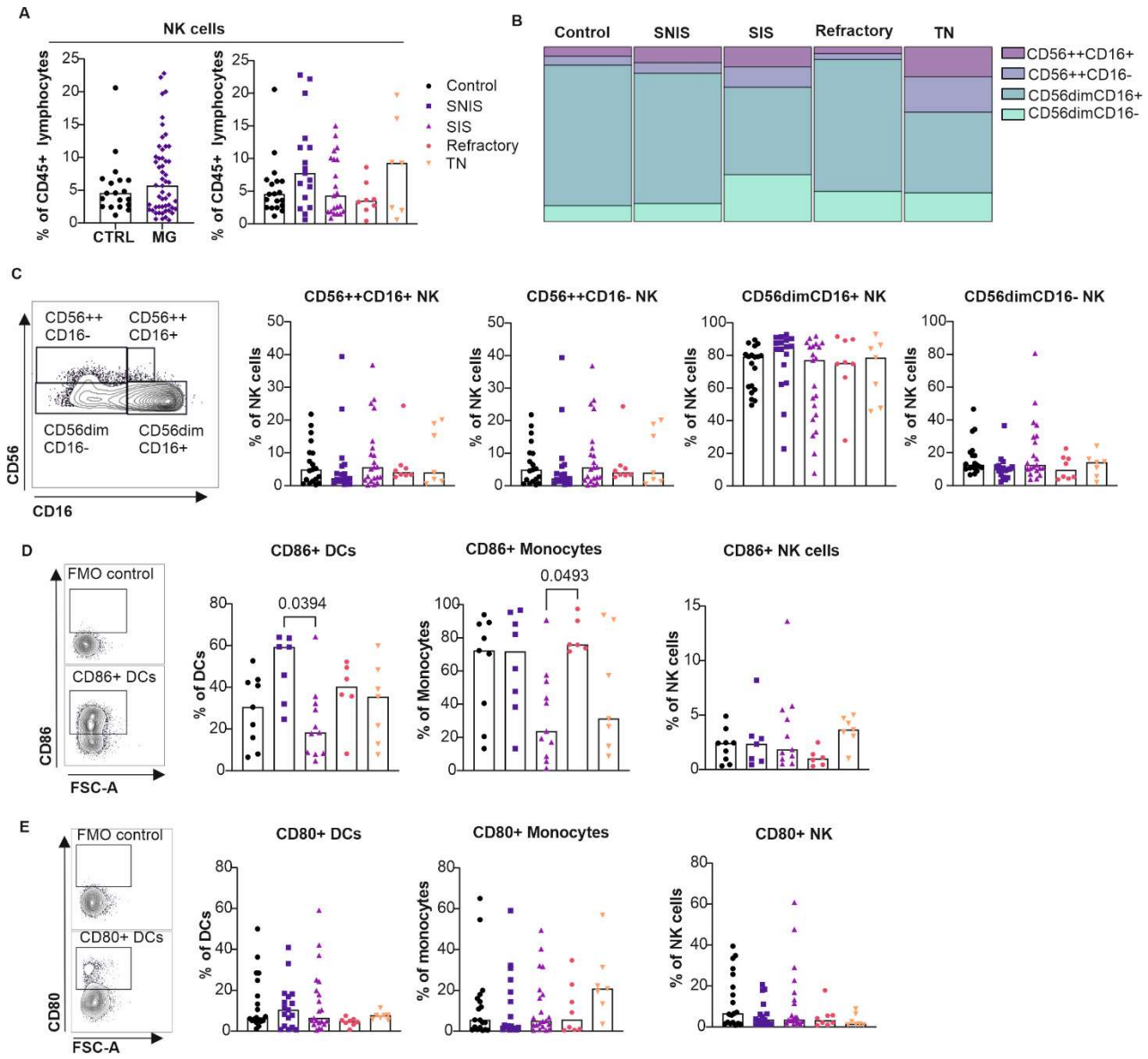

Supplementary Figure 5.

Fig. S5. NK cell subtyping, and CD80 and CD86 expression on myeloid cells in AChR-MG.

(A) Graphs showing frequencies of NK cells in control (n=18) compared to MG (n=48) and in subgroups; control (n=18), SNIS (n=17), SIS (n=19), refractory (n=6), TN (n=6). **(B)** Graph showing relative frequency of CD56brightCD16+, CD56brightCD16-, CD56dimCD16+ and CD56dimCD16- NK cells in subgroups; control (n=18), SNIS (n=17), SIS (n=19), refractory (n=6), TN (n=6). **(C)** Representative FACS plot demonstrating gating strategy for CD56brightCD16+, CD56brightCD16-, CD56dimCD16+ and CD56dimCD16- NK cells, gated on CD3-CD19-CD56+ live lymphocytes, and graphs showing frequencies of these populations

for subgroups; control (n=18), SNIS (n=17), SIS (n=19), refractory (n=6), TN (n=6). **(D)** FACS plot demonstrating gating strategy using an FMO for CD86 on DCs, and graphs showing CD86+ frequency in DCs, monocytes and NK cells for subgroups; control (n=18), SNIS (n=17), SIS (n=19), refractory (n=6), and TN (n=6). **(E)** FACS plots demonstrating gating strategy using an FMO for CD80 on DCs, and graphs showing CD80+ frequency in DC, monocytes and NK cells for subgroups; control (n=18), SNIS (n=17), SIS (n=19), refractory (n=6), and TN (n=6). Graphs show individual participant data, with bar representing median values. All comparisons are performed by student's t-test or one-way ANOVA with Tukey multiple comparison test (parametric data) or Mann-Whitney or Kruskal-Wallis with Dunn's multiple comparison test (non-parametric).

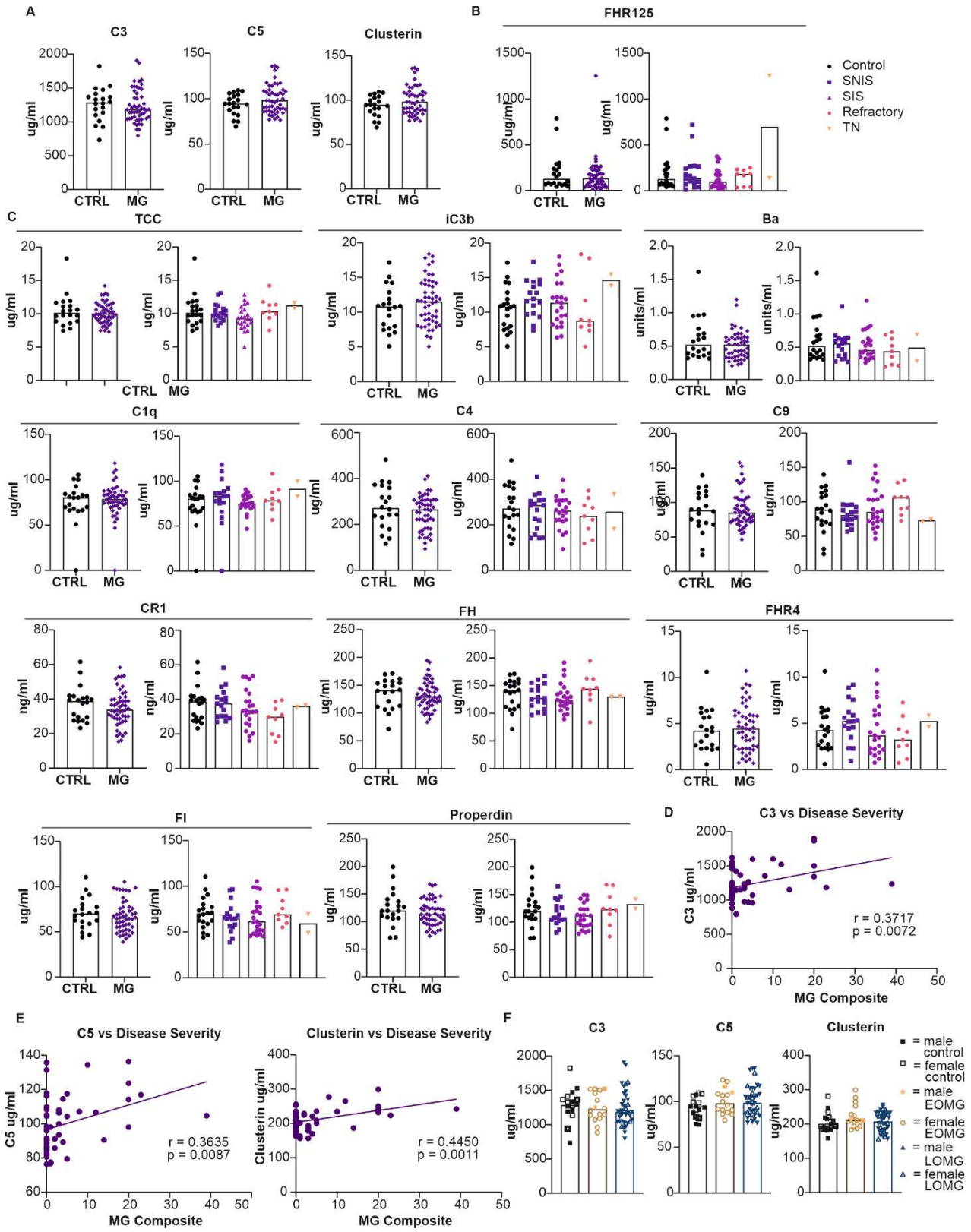

Supplementary Figure 6.

Fig. S6. Complement proteins in AChR-MG

(A) Graphs showing frequencies of C3, C5, and clusterin in control (n=20) compared to MG (n=52). **(B)** Graph showing frequency of FHR125 in control (n=20), compared to MG (n=52), and between subgroups control (n=20), SNIS (n=18), SIS (n=23), Refractory (n=9), and TN (n=2). **(C)** Graphs showing frequencies of TCC, iC3b, Ba, C1q, C4, C9, CR1, FH, FHR4, FI, and Properdin in control (n=20) compared to MG (n=52), and between subgroups control (n=20), SNIS (n=18), SIS (n=23), refractory (n=9), and TN (n=2). **(D)** Graph showing simple linear regression between C3 with disease severity (as measured by the MG Composite score) (n=56). **(E)** Graphs showing simple linear regression between C5 and clusterin with disease severity (as measured by the MG Composite score) (n=56). **(F)** Graphs showing C3, C5 and clusterin levels in control (n=20), compared to EOMG (n=16) and LOMG (n=38).

Graphs show individual participant data, with bar representing median values. All comparisons are performed by student's t-test or one-way ANOVA with Tukey multiple comparison test (parametric data) or Mann-Whitney or Kruskal-Wallis with Dunn's multiple comparison test (non-parametric). Correlation is calculated by Pearson (parametric) or Spearman correlation (non-parametric).

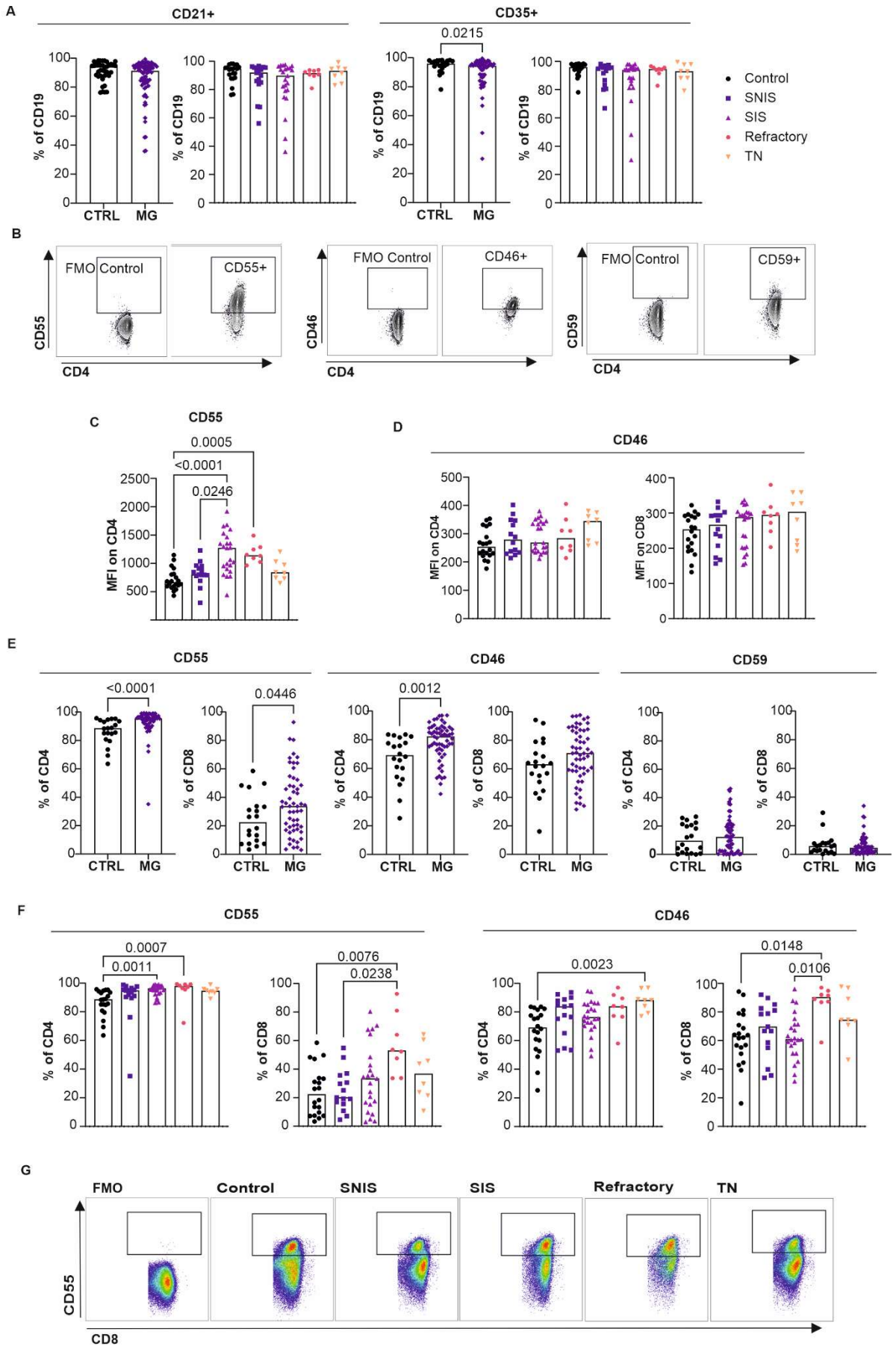

Supplementary Figure 7.

Fig. S7. Lymphocyte complement receptor expression in AChR-MG

(A) Graphs showing frequency of CD21+ and CD35+ B cells in control (n=20) compared to MG(n=56) and in subgroups control (n=20), SNIS (n=17), SIS (n=22), refractory (n=9), and TN (n=8). **(B)** FACS plots demonstrating gating strategy for CD55, CD46 and CD59 on CD4 T cells using FMO controls. **(C)** Graph showing CD55 expression on CD4 T cells in subgroups control (n=20), SNIS (n=15), SIS (n=23), refractory (n=8), and TN (n=8). **(D)** Graphs showing CD46 expression on CD4 and CD8 T cells in subgroups control (n=20), SNIS (n=15), SIS (n=23), refractory (n=8), and TN (n=8). **(E)** Graphs showing CD55+, CD46+ and CD59+ CD4 and CD8 T cells in control (n=20) compared to MG (n=54). **(F)** Graphs showing frequency of CD55+ and CD46+ CD4 and CD8 T cells in subgroups control (n=20), SNIS (n=15), SIS (n=23), refractory (n=8), and TN (n=8). **(G)** Representative FACS plots demonstrating CD55 expression on CD8 T cells in subgroups and FMO Control.

Graphs show individual participant data, with bar representing median values. All comparisons are performed by student's t-test or one-way ANOVA with Tukey multiple comparison test (parametric data) or Mann-Whitney or Kruskal-Wallis with Dunn's multiple comparison test (non-parametric).

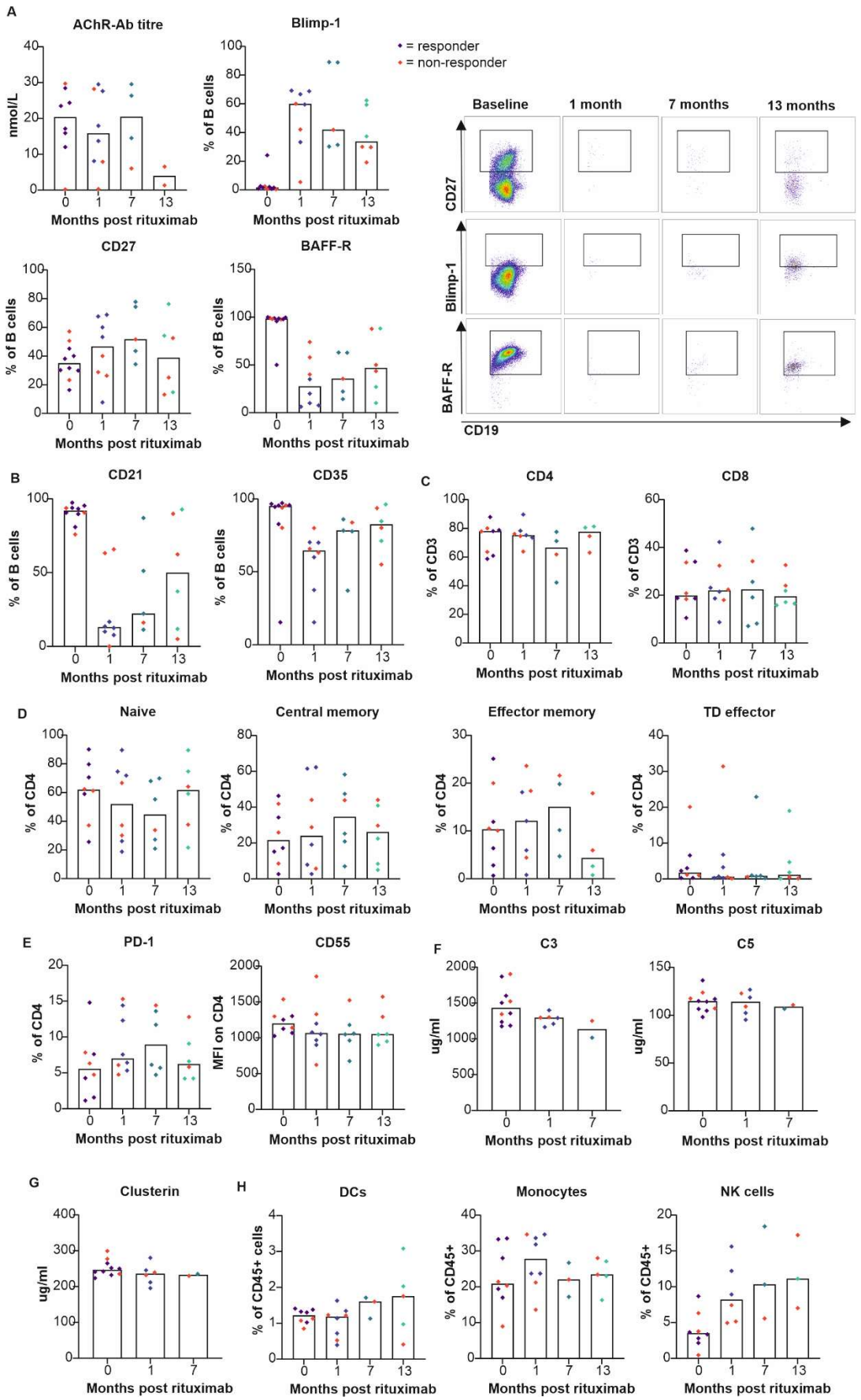

Supplementary Figure 8.

Fig. S8. Prospective changes seen following rituximab for refractory AChR-MG

(A) Graphs showing AChR tire and CD27+, Blimp-1+ and BAFF-R+ B cell frequency in the refractory group at baseline (n=8 AChR, n=10 B cells) and 1 month (n=8), 7 months (n= 4 AChR, n=6 B cells), and 13 months (n= 2 AChR, n=6 B cells) post rituximab, and representative FACS plots showing changes in CD27+, Blimp-1+ and BAFF-R+ B cell frequency. **(B)** Graphs showing CD21+ and CD35+ B cell frequency in the refractory group at baseline (n=10) and 1 month (n=8), 7 months (n=5), and 13 months (n=6) post rituximab. **(C)** Graphs showing CD4 and CD8 T cell frequency at baseline (n=10), to 1 month (n=8), 7 months (n=5), and 13 months (n=6) post rituximab. **(D)** Graphs showing naïve, central memory, effector memory and TD effector T cell frequency at baseline (n=10) and 1 month (n=8), 7 months (n=5), and 13 months (n=6) post rituximab. **(E)** Graphs showing PD-1+ CD4 T cell frequency and CD55 expression on CD4 T cells at baseline (n=10) and 1 month (n=8), 7 months (n=5), and 13 months (n=6) post rituximab. **(F)** Graphs showing C3 and C5 levels at baseline (n=10) and 1 month (n=6), and 7 months (n=2) post rituximab. **(G)** Graph showing changes to clusterin levels at baseline (n=10) and 1 month (n=6), and 7 months (n=2) post rituximab. **(H)** Graphs showing changes in monocyte, DC and NK cell frequency in the refractory group at baseline (n=10), to 1 month (n=8), 7 months (n=4), and 13 months (n=5) post rituximab.

Graphs show individual participant data, with bar representing median values. Red points denote “non-responders” to rituximab.

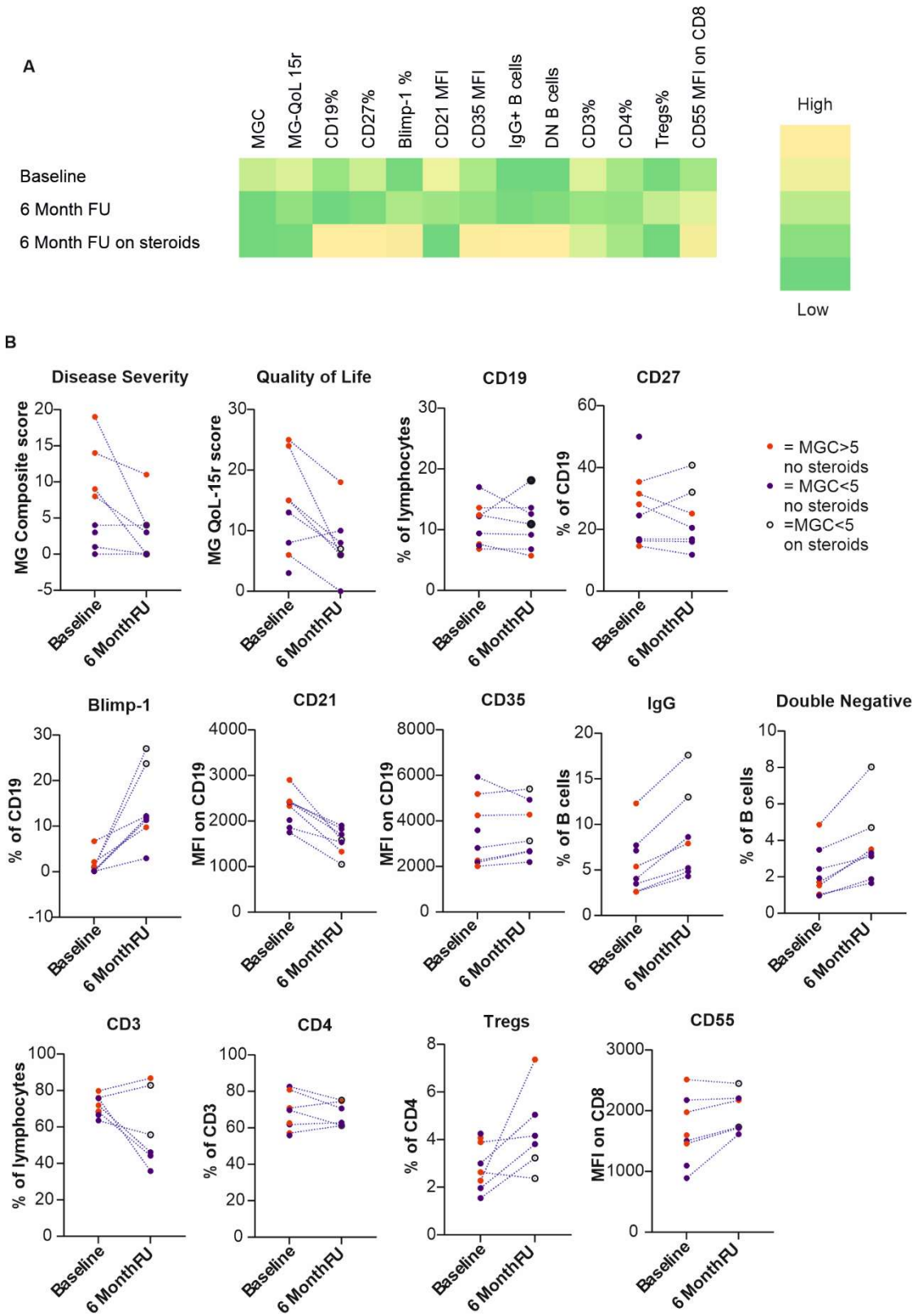

Supplementary Figure 9.

Fig. S9. Prospective six-month follow-up of treatment naïve AChR-MG

(A) Heatmap summarising changes in disease severity, quality of life, and frequencies of B cells, CD27+ and Blimp-1+ B cells, expression of CD21 and CD35 on B cells, frequencies of IgG+ and double negative B cells, CD3, CD4, and regulatory T cells, and expression of CD55 on CD8 T cells at baseline (n=8) to 6-month follow-up on not on steroids (n=5) and on steroids (n=2) in treatment naïve participants. **(B)** Graphs changes in disease severity, quality of life, and frequencies of B cells, CD27+ and Blimp-1+ B cells, expression of CD21 and CD35 on B cells, frequencies of IgG+ and double negative B cells, CD3, CD4, and regulatory T cells, and expression of CD55 on CD8 T cells at baseline (n=8) to 6-month follow-up on not on steroids (n=5) and on steroids (n=2) in treatment naïve participants. Graphs show individual participant data, with paired data connected via dotted line. Red circles indicate those with an MG Composite (MGC; disease severity) score over 5, empty circles indicate those on corticosteroids.

Supplementary Tables

Table S1. List of participants with gender, age, ethnicity and cohort

Participant	Gender	Age	Ethnicity	Cohort	EOMG / LOMG
1	Male	72	White British	Control	n/a
2	Female	75	White British	Control	n/a
3	Female	70	White British	Control	n/a
4	Male	66	White British	Control	n/a
5	Female	70	White British	Control	n/a
6	Male	20	African	Control	n/a
7	Female	72	White British	Control	n/a
8	Female	53	Asian	Control	n/a
9	Female	30	White British	Control	n/a
10	Male	42	White British	Control	n/a
11	Male	58	White British	Control	n/a
12	Female	71	White British	Control	n/a
13	Female	63	White British	Control	n/a
14	Female	77	White British	Control	n/a
15	Male	58	White British	Control	n/a
16	Male	61	White British	Control	n/a
17	Male	69	White British	Control	n/a
18	Male	63	Asian	Control	n/a
19	Male	66	White British	Control	n/a
20	Male	73	White British	Control	n/a
21	Female	63	White British	SNIS	LOMG

22	Male	77	White British	SNIS	LOMG
23	Male	68	White British	SNIS	LOMG
24	Female	53	White British	SNIS	EOMG
25	Female	79	White British	SNIS	EOMG
26	Male	77	White British	SNIS	LOMG
27	Male	75	White British	SNIS	LOMG
28	Female	28	White British	SNIS	EOMG
29	Female	64	White British	SNIS	LOMG
30	Male	60	White British	SNIS	LOMG
31	Male	75	White British	SNIS	LOMG
32	Male	78	White British	SNIS	LOMG
33	Female	57	Asian (Indian)	SNIS	LOMG
34	Female	36	White British	SNIS	EOMG
35	Male	79	White British	SNIS	LOMG
36	Male	67	White British	SNIS	EOMG
37	Female	70	White British	SNIS	LOMG
38	Female	40	White British	SIS	EOMG
39	Male	76	White British	SIS	LOMG
40	Male	78	White British	SIS	LOMG
41	Female	66	Eurasian	SIS	EOMG
42	Female	60	White British	SIS	EOMG
43	Male	75	White British	SIS	LOMG
44	Male	73	White British	SIS	LOMG
45	Male	73	White British	SIS	LOMG
46	Male	56	White British	SIS	EOMG

47	Male	74	White British	SIS	LOMG
48	Female	38	White British	SIS	EOMG
49	Male	75	White British	SIS	LOMG
50	Male	70	White British	SIS	LOMG
51	Male	65	White British	SIS	LOMG
52	Female	75	White British	SIS	LOMG
53	Male	73	White British	SIS	LOMG
54	Male	69	White British	SIS	LOMG
55	Female	76	White British	SIS	LOMG
56	Male	63	White British	SIS	LOMG
57	Male	71	White British	SIS	LOMG
58	Male	74	White British	SIS	LOMG
59	Male	65	White British	SIS	LOMG
60	Female	50	Black African	SIS	EOMG
61	Female	20	White British	Refractory	EOMG
62	Female	61	White British	Refractory	EOMG
63	Male	61	White British	Refractory	LOMG
64	Female	62	White British	Refractory	LOMG
65	Male	50	White British	Refractory	LOMG
66	Female	58	Asian (Hong-Kong Chinese)	Refractory	LOMG
67	Male	72	White British	Refractory	LOMG
68	Female	42	Black African	Refractory	EOMG
69	Male	64	White British	Refractory	LOMG
70	Male	54	White British	Refractory	LOMG
71	Female	42	White British	TN	EOMG

72	Female	26	Asian (Pakistani)	Naive	EOMG
73	Male	72	White British	Naive	LOMG
74	Female	69	White British	Naive	LOMG
75	Female	69	White British	Naive	LOMG
76	Male	69	White British	Naive	LOMG
77	Male	59	White British	Naive	LOMG
78	Male	64	White British	Naïve	LOMG

EOMG, early onset myasthenia gravis; LOMG, late onset myasthenia gravis; SIS, stable immunosuppressed; SNIS, stable, non-immunosuppressed; TN, treatment naive

Table S2. Antibodies used in flow cytometry staining

Fluorophore	Marker	Clone	Supplier	Catalog Number
AF488	Blimp-1	646702	R&D Systems	IC36081G
AF700	Ki67	Ki-67	Biolegend	350530
AF700	CXCR5	J252D4	Biolegend	356916
AF700	CD4	SK3	Biolegend	344622
APC	CD21	Bu32	Biolegend	254906
APC	CD59	p282	Biolegend	304712
APC	CD123	6H6	Biolegend	306012
APC	IL-10	JES3-19F1	Biolegend	506807
APC	CD3	BW264/56	Miltenyi Biotec	130-113-125
APC/Fire 750	CD24	ML5	Biolegend	311140
APC/Fire 750	CD56	5.1H11	Biolegend	362554
BV 650	CD19	HIB19	Biolegend	302238
BV421	IgG	M1310G05	Biolegend	410704
BV421	CCR7 (CD197)	G043H7	Biolegend	353208
BV421	CD66b	6/40c	Biolegend	392916
BV510	IgM	MHM-88	Biolegend	314522
BV510	CD279 (PD-1)	EH12.2H7	Biolegend	329932
BV510	CD45	HI30	Biolegend	304036
BV605	IgD	IA6-2	Biolegend	348232
BV605	CD45RA	HI100	Biolegend	304134
BV605	CD16	3G8	Biolegend	302040

BV605	CD3	UCHT1	Biolegend	300460
BV650	CD3	UCHT1	Biolegend	300468
BV650	CD19	HIB19	Biolegend	302238
BV711	CD274 (PD-L1)	29E.2A3	Biolegend	329722
BV711	CD25	BC96	Biolegend	302636
BV711	CD86	29E.2A3	Biolegend	329722
BV785	CD11c	3.9	Biolegend	301644
BV785	CD8	SK1	Biolegend	344740
BV785	CD11c	3.9	Biolegend	301644
BV785	CD19	HIB19	Biolegend	302240
FITC	FoxP3	206D	Biolegend	320106
FITC	CD14	M5E2	Biolegend	301804
PE Dazzle 594	CD27	M-T271	Biolegend	329732
PE Dazzle 594	CTLA-4 (CD152)	L3D10	Biolegend	349922
PE Dazzle 594	CD303 (BDCA-2)	201A	Biolegend	354226
PE.	CD35	E11	Biolegend	333406
PE.	CD55 (DAF)	JS11	Biolegend	311308
PE.	CD64	10.1	Biolegend	305008
PE.	IL-6	MQ2-13A5	Biolegend	501107
PeCy7	CD19	HIB19	Biolegend	302216
PeCy7	CD46 (MCP)	TRA-2-10	Biolegend	352408
PeCy7	CD80	2D10	Biolegend	305218
Pe Cy7	TNF-a	MAb11	Biolegend	502930

PeCy7	BAFF-R	11C1	Biolegend	316920
PerCP/Cy5.5	CD38	HIT-2	Biolegend	303522
PerCP/Cy5.5	CD4	OKT4	Biolegend	317428
PerCP/Cy5.5	HLA-DR	L243	Biolegend	307630
UV – 395	Live / dead	Zombie UV Fixable Viability Kit	Biolegend	423107

Table S3. Antibodies, standards and sample dilutions used in complement ELISA.

Assay	Capture antibody	Detection antibody	Protein	Detection range	Dilution factor
Ba	mAb D22/3 (Hycult)	mAb P21/15-HRP (Hycult)	Ba (Comptech)	8.5–550 ng/ml	1:4
iC3b	mAb clone 9	mAb bH6 -HRP (Hycult)	iC3b (Comptech)	23–1500 ng/ml	1:40
TCC	mAb aE11 (Hycult)	mAb E2 anti-C8-biotin	TCC	39–2500 ng/ml	1:40
C1q	mAb 9H10	Rabbit anti-C1q	C1q	23–1500 ng/ml	1:16000
C3	mAb 2898 (Hycult)	mAb clone 3-HRP (Hycult)	C3	31–2000 ng/ml	1:2000
C4	Rabbit anti-C4	Rabbit anti-C4-HRP	C4 (Comptech)	15–1000 ng/ml	1:4000
C5	mAb 10B6	mAb 4G2-HRP	C5	39–2500 ng/ml	1:500
C9	mAb B7	Rabbit anti-C9-biotin	C9	3–200 ng/ml	1:4000
Clusterin	mAb 2D5	mAb 4C7-HRP	Clusterin	31–2000 ng/ml	1:1000
sCR1	Rabbit anti-sCR1	mAb MBI35-HRP	sCR1	0.4–25 ng/ml	1:2

FH	mAb OX24	mAb 35H9-HRP	FH	15–1000 ng/ml	1:4000
FHR4	mAb 4E9	mAb clone 150-HRP	FHR4	15–1000 ng/ml	1:100
FHR125	mAb MBI125	clone 35H9-HRP	FHR125	156–10,000 ng/ml	1:100
FI	mAb 7B5	Rabbit anti-FI	FI	15–1000 ng/ml	1:500
Properdin	mAb 9.3.4 (Hycult)	mAb clone 2.9 (Hycult)	Properdin (Comptech)	6–400 ng/ml	1:1600

All antibodies were prepared in house unless stated otherwise specified for each analyte. mAb; monoclonal antibody, HRP, horseradish peroxidase, Comptech; Complement Technology Inc.,TCC, terminal complement complex; FH, factor H; FHR125, FH-related proteins 1, 2, and 5; FHR4, FH-related protein 4; sCR1, soluble complement receptor type 1; FI, factor I.